

Joint Service Caching and Computing Resource Allocation for Edge Computing-Enabled Networks

Mingun Kim, Hewon Cho, Ying Cui, *Member, IEEE*, and Jemin Lee, *Member, IEEE*

Abstract—In this paper, we consider the service caching and the computing resource allocation in edge computing (EC) enabled networks. We introduce a random service caching design considering multiple types of latency sensitive services and the base stations (BSs)' service caching storage. We then derive a successful service probability (SSP). We also formulate a SSP maximization problem subject to the service caching distribution and the computing resource allocation. Then, we show that the optimization problem is nonconvex and develop a novel algorithm to obtain the stationary point of the SSP maximization problem by adopting the parallel successive convex approximation (SCA). Moreover, to further reduce the computational complexity, we also provide a low complex algorithm that can obtain the near-optimal solution of the SSP maximization problem in high computing capability region. Finally, from numerical simulations, we show that proposed solutions achieve higher SSP than baseline schemes. Moreover, we show that the near-optimal solution achieves reliable performance in the high computing capability region. We also explore the impacts of target delays, a BSs' service cache size, and an EC servers' computing capability on the SSP.

I. INTRODUCTION

With the growing popularity of mobile applications and the IoT technology, the demand for computation intensive and latency sensitive services such as virtual reality is also increasing. It is hard for mobile users to meet the required deadline of the computation task, due to the limited battery capacity and the low computing capability of the mobile user. One promising solution for tackling this issue is the edge computing (EC) technology, which utilizes the computing capability at the network edge such as the base stations (BSs) [2]. By applying the EC, the computation task of a mobile user is offloaded to its nearby BS. Once the computation is completed, the computation result is transmitted to the user, which results in lower latency compared to the local computing.

To reduce the cost of executing the task at the EC server, the content caching has been considered in the EC-enabled networks. In the content caching, each BS caches the computation

results of certain tasks frequently requested by users, so a BS can directly transmit the computation results of the requested task to the user without executing the task at the EC server again. Therefore, the execution cost at the EC server can be reduced.

However, when users often use computation intensive applications including the cognitive assistance and virtual/augmented reality, different service software is required, and a BS that caches certain service software can directly execute a task for the service. Therefore, to tackle these issues, service caching at the network edge, i.e., caching the software of services that are frequently requested by mobile users at BSs, has been recently introduced [3]. Supported by the service caching, a BS that caches certain service software can directly compute a computation task that belongs to the certain service. Due to the limited storage resource, it is hard for a BS to cache all service software. Therefore, it is critical to optimally select the service software to be cached at each BS.

There have been several works on optimal communication and computing resource allocations and task offloading decisions in EC enabled networks [4]–[7]. For example, in [4]–[6], the communication and computing resource allocations and task offloading decisions are jointly optimized to minimize the energy consumption and latency for computing and transmitting tasks. In [7], the communication resource allocation and task offloading decisions are jointly optimized to minimize the energy consumption of computing and transmitting tasks. However, in [4]–[7], the authors assume that the numbers and locations of BSs and users are fixed, which makes their solutions ineffective when the network setup changes. Moreover, it can be unrealistic for a control tower to know all locations and channels of all BSs and users. Recently, randomly distributed BSs and users have been considered in several works which analyze the communication and computation latency in EC enabled networks [8]–[10]. Specifically, [8], [9] consider multi tier heterogeneous networks and [10] studies single tier networks. Nevertheless, in the aforementioned works [4]–[10], the authors implicitly assume that all service software can be cached at each BS. This assumption is unrealistic due to the limited storage resource at a BS.

As tasks belonging to different services have possibly distinct computation workloads, service caching should be jointly optimized with the computing resource allocation. There have been some recent works on the joint optimization of the service caching, communication and computing resource allocations, and task offloading decisions in EC enabled networks [3], [11]–[15]. For example, in [3], [11]–[13], the service caching

The material in this paper was presented, in part, at the IEEE Global Communications Conference, Taipei, Taiwan, December, 2020 [1].

M. Kim and H. Cho are with the Department of Electrical Engineering and Computer Science, Daegu Gyeongbuk Institute of Science and Technology, Daegu, 42988, South Korea (e-mail: {alsrjs1807, nb00040}@dgist.ac.kr).

Y. Cui is with the Department of Electronic Engineering, Shanghai Jiao Tong University, Shanghai 200240, China (e-mail: cuiying@sjtu.edu.cn).

J. Lee is with the Department of Electrical and Computer Engineering, Sungkyunkwan University (SKKU), Suwon 16419, Republic of Korea (e-mail: jemin.lee@skku.edu).

and task offloading decisions are jointly optimized to minimize the energy consumption and latency for computing and transmitting tasks. In [14], an online algorithm is presented for the dynamic service caching with arbitrary service request patterns. In [15], the authors optimize communication and computing resource allocations together with the service caching and task offloading decisions. However, in most works on service caching in EC enabled networks such as [3], [11]–[15], fixed numbers of BSs and users with fixed locations are considered, which can be impractical for wireless networks of diverse deployments and mobile users with varying locations. On the other hand, some works such as [16] consider random distributions of BSs and users for content caching by considering data intensive services rather than computation intensive services.

This motivates us to optimize the service caching and the computing resource allocation with randomly distributed BSs and users in the large-scale networks for randomly distributed BSs and users. Each user randomly requests a computation task that belongs to a particular service. Each BS has an EC server, and caches service software. We investigate two service time cases at the EC server: the random service time (RT) and the deterministic service time (DT) cases. Since BSs and users are randomly distributed in the networks, we first analyze the average networks performance, i.e., the successful service probability (SSP), which is the probability of completing the service request, computation, and reception of the computation result are completed within their respective target delays. Then, we formulate the SSP maximization problem subject to the service caching and the computing resource allocation and obtain the stationary point of the SSP maximization problem. The main contributions of this paper can be summarized as follows.

- We newly provide the closed form expression of the approximated SSP for both the RT and the DT cases using stochastic geometry and queuing theory. The approximated SSP for the RT case is a differential function, and the approximated SSP for the DT case is converted to a differential form using the Hausdorff approximation [17] for tractability in the later SSP optimization.
- We jointly optimize the service caching and the computing resource allocation to maximize the SSP for both the RT and the DT cases in the large-scale networks for randomly distributed BSs and users. To the best of our knowledge, this is the first time that jointly optimizes the service caching and computing resource allocation for randomly distributed BSs and users.
- Since the formulated SSP maximization problem is a challenging nonconvex problem with a large number of variables, we propose a parallel iterative algorithm to obtain a stationary point based on parallel successive convex approximation (SCA) [18]. Note that the parallel SCA yields lower computational complexity than the conventional SCA.
- To further reduce the computational complexity, we also develop a low complex algorithm that obtains a near-optimal solution of the SSP maximization problem for

both the RT and the DT cases by using the asymptotically optimal solution obtained for the infinite computing capability case.

- From numerical results, we show the superiority of the proposed algorithms compared to baseline schemes. We also reveal the impacts of BSs' service cache size, computing capability of the EC server, and target delays of each service on the SSP.

The remainder of this paper is organized as follows. Section II describes the system model. Section III analyzes the SSP for both the RT and the DT cases. Section IV formulates the SSP maximization problem in the EC enabled network. Moreover, iterative algorithm to obtain the stationary point of SSP maximization problem is proposed. We then develop the iterative algorithm with low complexity to obtain the near-optimal solution of SSP the maximization problem in Section V. Numerical results are provided in Section VI. Finally, the conclusions are given in Section VII.

II. SYSTEM MODEL

In this section, we present the system model of an edge computing (EC)-enabled network with the randomly distributed base stations (BSs) and users. Each user requests a computation task that belongs to service among multiple types of services, which can be computed by the service software cached at the BSs.

A. Network Model

We consider an EC enabled network which consists of single antenna BSs and single antenna users as shown in Fig. 1. The locations of BSs and users are modeled as independent homogeneous Poisson point processes (PPPs) Φ_{bs} and Φ_u , with spatial densities λ_{bs} and λ_u , respectively. Each BS is equipped with a cache and an EC server. Therefore, each BS has both caching and computing capabilities, while each user has neither caching nor computing capabilities¹. The computing capability of each BS is denoted by $F_{bs} > 0$ [number of CPU cycles per second], and the transmit power of BSs and users are denoted by P_{bs} and P_u [Watt], respectively. We consider both uplink and downlink transmissions operating in the time-division duplexing (TDD) mode. The channel bandwidth is W [Hz], and each channel is reused in every κ cell. As a consequence, the distribution of interfering BSs can be approximated into a PPP $\tilde{\Phi}_{bs}$ with spatial density $\frac{\lambda_{bs}}{\kappa}$ [19]. We consider both path loss and small scale fading. Due to path loss, a transmitted signal with distance x is attenuated by a factor $x^{-\alpha}$, where $\alpha > 2$ is the path loss exponent. For small scale fading, we assume Rayleigh fading channels.

We consider N latency sensitive services, denoted by $\mathcal{N} \triangleq \{1, 2, \dots, N\}$. We assume each user randomly requests latency sensitive service $n \in \mathcal{N}$ with probability $p_n \in [0, 1]$, where $\sum_{n \in \mathcal{N}} p_n = 1$. To provide service n to the user, a certain computation task (i.e., task n) needs to be executed by its

¹Note that the proposed algorithm in this paper can also be used for the case where not only BSs but also users have both the caching and computing capabilities. This can be done by adding the optimization parameters and the constraints of the user in a similar way to the ones for BSs.

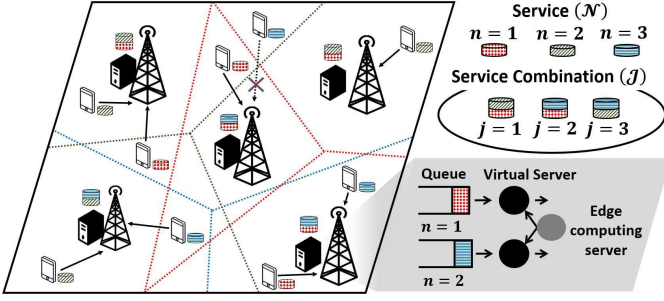


Fig. 1. System model where BSs, equipped with a EC server, have two different service software (i.e., $K = 2$) among three different services (i.e., $N = 3$). Each Voronoi cell (in the same color as the service) represents the BS coverage for each service.

service software. Each task n is characterized by three task parameters, i.e., the size of input data $S_n^{(i)} > 0$ [bits], the size of computation result $S_n^{(o)} > 0$ [bits], and the size of computation workload f_n [number of CPU cycles].

We consider a discrete time model, where time is divided into discrete slots. Specifically, in each time slot, each user randomly decides whether to request a service or not with probability $p_s \in [0, 1]$. Once the user decides to request a service, we assume that the user randomly requests one service among \mathcal{N} . Here, we define p_n as the probability that a user requests service $n \in \mathcal{N}$, where $\sum_{n \in \mathcal{N}} p_n = 1$. Note that p_n is the long-term average of users' service request, i.e., the service popularity in the large-scale EC-enabled networks. Regarding of the association, we consider the service centric association rule, where a user requesting a task n associates with the nearest BS caching the service software n . When user sends a service request to its serving BS, the BS executes the computation task of the requested service. After computing the task, the BS transmits the computation result to the user. However, when the user is associated with the other BS in present, the BS transmits the computation result to the user through the other BS associated with the user.

B. Service Caching and Computation Model

In a practical EC enabled network, each EC server has limited computing capability and caching storage, so the only limited amount of service software can be cached [3]. Therefore, each BS can cache the different amount of service software within its limit of caching storage. Let us define Ω_{bs} and $\Omega_n, n \in \mathcal{N}$ as the BSs' cache storage and the required storage size to cache the service software n , respectively. Then, we can obtain the set of possible service combinations \mathcal{J} that satisfy the following constraints.

$$\sum_{k \in \mathcal{J}} \Omega_k \leq \Omega_{bs}. \quad (1)$$

However, for analytical tractability, we consider that the same amount of service software is cached at each BS. Then, without loss of generality, we assume that each BS caches $K (\leq N)$ service software of the same size. Hence, there exist $J \triangleq \binom{N}{K}$ different service combinations that can be cached in a BS. Let $\mathcal{J} \triangleq \{1, 2, \dots, J\}$ denote the index set of all possible service combinations.

We consider a *random service caching* design, where a service combination is randomly adopted by each BS with a certain probability. The probability that service combination j is cached in a BS is denoted by a_j , where

$$a_j \geq 0, \quad j \in \mathcal{J}, \quad (2)$$

$$\sum_{j \in \mathcal{J}} a_j = 1. \quad (3)$$

Here, we denote $\mathbf{a} \triangleq (a_j)_{j \in \mathcal{J}}$ as the service caching distribution. Furthermore, we define the set of service combinations which include service software n as \mathcal{J}_n . From this, the probability that service software n is cached at a BS, denoted by T_n , where

$$T_n = \sum_{j \in \mathcal{J}_n} a_j, \quad n \in \mathcal{N}, \quad (4)$$

$$0 \leq T_n \leq 1, \quad n \in \mathcal{N}, \quad (5)$$

$$\sum_{n \in \mathcal{N}} T_n = K. \quad (6)$$

Here, we denote $\mathbf{T} \triangleq (T_n)_{n \in \mathcal{N}}$ as the service probability distribution. Note that the random service caching adopted in this paper is analogous to the random caching considered in [16].

We assume that each EC server has K virtual servers with different computing capabilities by applying hyper threading technology and asymmetric heterogeneous computing [20]. Each virtual server has a queue with infinite capacity and can execute different service software cached in the BS. In other words, we consider the EC server consisting of K queues and K virtual servers, and each cached service is executed in a different set of the single queue and single virtual server. Regarding the service time at the server, we consider two cases: 1) random service time (RT) case and 2) deterministic service time (DT) case. Specifically, the service time is modeled as an exponential random variable in the RT case, and as constant time in the DT case. Those two models are the ones, generally used in existing works². The service time is denoted by $D_{n,k}^{(Q)}, k \in \{m, d\}$, where 'm' and 'd' indicate the RT and DT cases, respectively. We adopt the first input first output (FIFO) discipline at each queue and virtual server. The computing capability assigned for executing service software n at the virtual server of the BS which caches service combination j , is denoted by $b_{n,j} F_{bs}$, where

$$b_{n,j} \geq 0, \quad j \in \mathcal{J}, \quad n \in \mathcal{N}_j, \quad (7)$$

$$\sum_{n \in \mathcal{N}_j} b_{n,j} = 1, \quad j \in \mathcal{J}. \quad (8)$$

Here, \mathcal{N}_j is the set of service software contained in combination j . We denote $\mathbf{b} \triangleq (b_{n,j})_{n \in \mathcal{N}, j \in \mathcal{J}}$ as the computing resource allocation.

²For example, the exponential distribution is used to model the service time at servers (e.g., edge and cloud-edge servers [21], [22], and the virtual machine [23]), and proven as a realistic model from the measurements of video computation times at YouTube [24]. The constant service time is also used for the edge computing system [25], [26] and the weather monitoring system [27].

C. Communication Model

Each user first transmits the service request message to its serving BS, corresponding to the uplink transmission. Without loss of generality, we assume that a typical user, denoted by u_o , is located at the origin, and the serving BS of u_o is denoted by $B_o^{(U)}$. We consider the interference limited environment when users using the same frequency band as u_o act as the interferer. Then, the maximum achievable uplink data rate for $B_o^{(U)}$ at u_o , denoted by $R^{(U)}$, is given by

$$R^{(U)} = \frac{W}{\kappa} \log_2 \left(1 + \frac{|h_{o,o}^{(U)}|^2 (d_{o,o}^{(U)})^{-\alpha}}{\sum_{l \in \Psi_{u_o}} |h_{l,o}^{(U)}|^2 (d_{l,o}^{(U)})^{-\alpha}} \right), \quad (9)$$

where Ψ_{u_o} is the locations of interfering users with respect to (w.r.t.) u_o . Here, $d_{l,t}^{(U)}$ and $h_{l,t}^{(U)}$ represent the distance and small scale fading channel gain of the link between u_l and B_t , respectively. Moreover, the uplink transmission time of u_o 's service request n is $D_n^{(U)} = \frac{S_n^{(i)}}{R^{(U)}}$.

Once $B_o^{(U)}$ finishes the computation of the service requested by u_o , it transmits the computation results to u_o or the BS associated with u_o at present. We denote $B_o^{(D)}$ as the BS associated with u_o at present. We assume that the transmission time between $B_o^{(U)}$ and $B_o^{(D)}$ is negligible due to the high capacity wired backhaul. Similar to the uplink scenario, BSs that use the same frequency band as $B_o^{(D)}$ act as the interferer. Then, the maximum achievable data rate for u_o at $B_o^{(D)}$, denoted by $R^{(D)}$, is given by

$$R^{(D)} = \frac{W}{\kappa} \log_2 \left(1 + \frac{|h_{o,o}^{(D)}|^2 (d_{o,o}^{(D)})^{-\alpha}}{\sum_{k \in \tilde{\Phi}_{bs}} |h_{o,k}^{(D)}|^2 (d_{o,k}^{(D)})^{-\alpha}} \right). \quad (10)$$

Then, the downlink transmission time of u_o 's computation result for service n is $D_n^{(D)} = \frac{S_n^{(o)}}{R^{(D)}}$.

D. Performance Metric

To satisfy that latency sensitive services require that the uplink transmission, computation, and downlink transmission are completed within their respective target delays as in [28], [29], we introduce a successful service probability (SSP), denoted by $\mathcal{P}(\mathbf{a}, \mathbf{b})$, as the performance metric, given as³

$$\mathcal{P}_k(\mathbf{a}, \mathbf{b}) = \sum_{n \in \mathcal{N}} p_n \mathbb{P} \left[D_n^{(U)} \leq \gamma_n^{(U)}, D_{n,k}^{(Q)} \leq \gamma_n^{(Q)}, \right. \\ \left. D_n^{(D)} \leq \gamma_n^{(D)} \right], k \in \{m, d\}, \quad (11)$$

where $\gamma_n^{(U)}$, $\gamma_n^{(Q)}$, and $\gamma_n^{(D)}$ are the target delays for uplink transmission, computation, and downlink transmission, respectively. Here, $D_n^{(U)}$, $D_{n,k}^{(Q)}$, $k \in \{m, d\}$, and $D_n^{(D)}$ can be correlated with each other, especially when the serving BS in uplink and downlink transmission, i.e., $B_o^{(U)}$, and $B_o^{(D)}$ are the same. However, for analytical tractability, we assume

that they are independent⁴, and hence, the SSP in (11) can be approximately expressed as

$$\tilde{\mathcal{P}}_k(\mathbf{a}, \mathbf{b}) = \sum_{n \in \mathcal{N}} p_n \mathbb{P} \left[D_n^{(U)} \leq \gamma_n^{(U)} \right] \mathbb{P} \left[D_{n,k}^{(Q)} \leq \gamma_n^{(Q)} \right] \\ \times \mathbb{P} \left[D_n^{(D)} \leq \gamma_n^{(D)} \right], k \in \{m, d\}. \quad (12)$$

III. SUCCESSFUL SERVICE PROBABILITY ANALYSIS

In this section, we analyze the SSP in both RT and DT cases. We first derive the successful uplink transmission probability (SUTP), the successful downlink transmission probability (SDTP) and the successful computation probability (SCPP). We then present the SSP.

A. Successful Uplink and Downlink Transmission Probabilities

In this subsection, we derive the SUTP and the SDTP when a user requests a task n and receives a computation result of the service n from its associated BS. For analytical tractability, we introduce the following assumption.

Assumption 1: The location of uplink interfering users w.r.t. the typical user follows the PPP.

Since one user exists in each cell and the user requests the task with probability p_s , the locations of interfering users are determined by thinning, dependent on BSs' locations. Therefore, the location of uplink interfering users does not follow a PPP. However, according to [30], it has been shown that this dependence is weak and can be negligible.

From Assumption 1, the distribution of uplink interfering users can be approximated to a PPP with spatial density $\frac{p_s \lambda_{bs}}{\kappa}$. Therefore, the SUTP of the user requesting a service n , denoted by $P_n^{(U)}(\mathbf{a})$, is given by [31]

$$P_n^{(U)}(\mathbf{a}) = \mathbb{P} \left[R^{(U)} \geq \frac{S_n^{(i)}}{\gamma_n^{(U)}} \right] \\ = \frac{T_n}{T_n + \frac{p_s}{\kappa} Z(\beta_n^{(U)}, \alpha, 0)}, \quad n \in \mathcal{N}, \quad (13)$$

where $Z(a, b, c) \triangleq a^{2/b} \int_{(c/a)^{2/b}}^{\infty} \frac{1}{1+u^{b/2}} du$ and $\beta_n^{(U)} \triangleq \frac{\kappa S_n^{(i)}}{2^w \gamma_n^{(U)}} - 1$.

After computing the requested service of the user, the BS transmits the computation result to the user. Hence, the SDTP of a BS transmitting the computation result of service n , denoted by $P_n^{(D)}(\mathbf{a})$, is given by [31]

$$P_n^{(D)}(\mathbf{a}) = \mathbb{P} \left[R^{(D)} \geq \frac{S_n^{(o)}}{\gamma_n^{(D)}} \right] \\ = \frac{T_n}{T_n \left(1 + \frac{p_s}{\kappa} Z(\beta_n^{(D)}, \alpha, 1) \right) + (1 - T_n) \frac{p_s}{\kappa} Z(\beta_n^{(D)}, \alpha, 0)}, \quad (14)$$

for $n \in \mathcal{N}$, where $\beta_n^{(D)} \triangleq \frac{\kappa S_n^{(o)}}{2^w \gamma_n^{(D)}} - 1$.

³Note that our work can be easily extended to the case where the target delays are optimized for maximizing the SSP.

⁴Note that there exists a performance between among the SSPs in (11) and (12) due to the independence assumption. However, in Section VI, we show that the approximation error is small enough to be ignored.

$$\tilde{P}_m(\mathbf{a}, \mathbf{b}) = \sum_{n \in \mathcal{N}} \frac{p_n T_n \sum_{j \in \mathcal{J}_n} a_j \left(1 - e^{-b_{n,j} J_n + \lambda_n(\mathbf{a}) \gamma_n^{(Q)}}\right)}{D_n T_n^2 + E_n T_n + A_n C_n}. \quad (22)$$

$$\tilde{P}_d(\mathbf{a}, \mathbf{b}) = \sum_{n \in \mathcal{N}} \frac{p_n T_n}{D_n T_n^2 + E_n T_n + A_n C_n} \sum_{j \in \mathcal{J}_n} a_j \left(1 - \frac{\lambda_n(\mathbf{a})}{b_{n,j} \mu_n}\right) \sum_{\xi=0}^{\lfloor J_n \rfloor} \frac{(\lambda_n(\mathbf{a}))^\xi \left(\frac{\xi}{b_{n,j} \mu_n} - \gamma_n^{(Q)}\right)^\xi e^{\lambda_n(\mathbf{a}) \left(\gamma_n^{(Q)} - \frac{\xi}{b_{n,j} \mu_n}\right)}}{\xi! \left(1 + e^{-\delta(\xi - b_{n,j} J_n)}\right) e^{-\delta(\xi - b_{n,j} J_n)}}. \quad (23)$$

B. Successful Computation Probability

In this subsection, we derive the SCPP in both the RT and DT cases. Since we adopt the service centric association rule, the task arrivals at each BS is derived in the following proposition.

Proposition 1: The arrivals of task n at a BS that caches the service software n can be modeled as a Poisson process (PP) Φ_n with an arrival rate $\lambda_n(\mathbf{a}) = \mathbb{E}[N_n] P_n^{(U)}(\mathbf{a})$.

Proof: By applying the service centric association rule, the mean number of users requesting the task n to a BS is given by $\mathbb{E}[N_n] = 1 + \frac{1.28 p_n p_s \lambda_u}{T_n \lambda_{bs}}$ [31]. Note that $\mathbb{E}[N_n]$ is independent of service combination j cached at the BS. This is because the mean number of users associated with the BS is dependent on whether the BS has service software n or not. Moreover, each user requests a task independently, and the input data of task n is transmitted successfully to the BS with probability $P_n^{(U)}(\mathbf{a})$ in (13). As a result, the task arrivals are modeled as PP with an arrival rate $\lambda_n(\mathbf{a}) = \mathbb{E}[N_n] P_n^{(U)}(\mathbf{a})$ [10]. ■

When the input data of task n arrives at the BS that caches the service combination j , the service n is scheduled at the BS's virtual server, and the computing capability $b_{n,j} F_{bs}$ is assigned for the computing service n . To guarantee the stability of the queue, we have the following constraint:

$$b_{n,j} \mu_n \geq \lambda_n(\mathbf{a}), \quad n \in \mathcal{N}, j \in \mathcal{J}, \quad (15)$$

where $\mu_n = \frac{F_{bs}}{T_n}$ is the maximum service rate at the virtual server for service n . Note that the condition in (15) guarantees that the arrival rate of task n is smaller than the service rate of the virtual server assigned for service n . Then, we denote $P_{n,j,k}^{(Q)}(\mathbf{a}, \mathbf{b})$, $k = \{m, d\}$ as the SCPP of service n at the BS that caches service combination j , which is given by

$$P_{n,j,k}^{(Q)}(\mathbf{a}, \mathbf{b}) = \mathbb{P} \left[D_{n,k}^{(Q)} \leq \gamma_n^{(Q)} \mid j \in \mathcal{J}_n \right], n \in \mathcal{N}. \quad (16)$$

Now, from (16), we derive the SCPP of service n for RT and DT cases.

1) *Random Service Time Case:* For the RT case, the service time of the virtual server is modeled as an exponential random variable. Since the task arrivals follow PP, we can model the computing process as the M/M/1 queue. Therefore, by applying the probability density function (PDF) of sojourn time in M/M/1 queue [32], the SCPP of service n at the BS that caches the service combination j is given by

$$P_{n,j,m}^{(Q)}(\mathbf{a}, \mathbf{b}) = 1 - e^{-(b_{n,j} \mu_n - \lambda_n(\mathbf{a})) \gamma_n^{(Q)}}, \quad n \in \mathcal{N}. \quad (17)$$

2) *Deterministic Service Time Case:* For the DT case, we can model the computing process as the M/D/1 queue with constant service time. Hence, by applying the cumulative

distribution function (CDF) of sojourn time in the M/D/1 queue [33], the SCPP of service n at the BS that caches the service combination j is given by

$$P_{n,j,d}^{(Q)}(\mathbf{a}, \mathbf{b}) = \sum_{\xi=0}^{\lfloor \gamma_n^{(Q)} \mu_n \rfloor} \frac{\mathbb{1} \left(b_{n,j} < D_{n,d}^{(Q)} b_{n,j} \mu_n \right) (\lambda_n(\mathbf{a}))^\xi}{\left(1 - \frac{\lambda_n(\mathbf{a})}{b_{n,j} \mu_n}\right)^{-1}} \times \frac{e^{\lambda_n(\mathbf{a}) \left(\gamma_n^{(Q)} - \frac{\xi}{b_{n,j} \mu_n}\right)}}{\left(\frac{\xi}{b_{n,j} \mu_n} - \gamma_n^{(Q)}\right)^{-\xi} \xi!}, n \in \mathcal{N}, \quad (18)$$

where $\lfloor x \rfloor$ is the floor function which gives the greatest integer less than or equal to x and $\mathbb{1}(A)$ is the indicator function which gives the value 1 if the condition A is satisfied and the value 0 otherwise. In (18), the indicator function can be tightly bounded by the logistic sigmoid function using the Hausdorff approximation [17], as follows:

$$\mathbb{1} \left(b_{n,j} < D_{n,d}^{(Q)} b_{n,j} \mu_n \right) \approx \frac{e^{-\delta(\xi - \gamma_n^{(Q)} b_{n,j} \mu_n)}}{\left(1 + e^{-\delta(\xi - \gamma_n^{(Q)} b_{n,j} \mu_n)}\right)}, \quad (19)$$

where δ is the cut radius of the sigmoid function. Note that the gap between the original indicator function and the logistic sigmoid function is very small for the large positive value of cut radius $\delta \gg 0$, and can be ignored. Hence, the SCPP in (18) can be approximated to a differentiable form such as $\tilde{P}_{n,j,d}^{(Q)}(\mathbf{a}, \mathbf{b})$, given by

$$\tilde{P}_{n,j,d}^{(Q)}(\mathbf{a}, \mathbf{b}) = \sum_{\xi=0}^{\lfloor \gamma_n^{(Q)} \mu_n \rfloor} \frac{\left(1 - \frac{\lambda_n(\mathbf{a})}{b_{n,j} \mu_n}\right) e^{\lambda_n(\mathbf{a}) \left(\gamma_n^{(Q)} - \frac{\xi}{b_{n,j} \mu_n}\right)}}{\left(\frac{\xi}{b_{n,j} \mu_n} - \gamma_n^{(Q)}\right)^{-\xi} (\lambda_n(\mathbf{a}))^{-\xi}} \times \frac{e^{-\delta(\xi - \gamma_n^{(Q)} b_{n,j} \mu_n)}}{\xi! \left(1 + e^{-\delta(\xi - \gamma_n^{(Q)} b_{n,j} \mu_n)}\right)}, n \in \mathcal{N}. \quad (20)$$

Later in Section VI, we will show that the approximation error is small enough to be ignored.

C. Successful Service Probability

The SSP in (12) can be represented as

$$\tilde{P}_k(\mathbf{a}, \mathbf{b}) = \sum_{n \in \mathcal{N}} p_n P_n^{(U)}(\mathbf{a}) P_n^{(D)}(\mathbf{a}) \sum_{j \in \mathcal{J}_n} \frac{a_j}{T_n} \tilde{P}_{n,j,k}^{(Q)}(\mathbf{a}, \mathbf{b}), \quad (21)$$

for $k \in \{m, d\}$, where $P_n^{(U)}$ and $P_n^{(D)}$ are in (13) and (14), respectively. Here, $\tilde{P}_{n,j,k}^{(Q)}(\mathbf{a}, \mathbf{b})$ is $P_{n,j,m}^{(Q)}(\mathbf{a}, \mathbf{b})$ in (17) for $k = m$ and $\tilde{P}_{n,j,d}^{(Q)}(\mathbf{a}, \mathbf{b})$ in (20) for $k = d$.

By substituting (13), (14), (17), and (20) into (21), the SSPs for the RT and DT cases are respectively given by (22) and (23), as shown on the top at this page, where $A_n = \frac{p_s}{\kappa} Z(\beta_n^{(U)}, \alpha, 0)$, $B_n = \frac{p_s}{\kappa} Z(\beta_n^{(D)}, \alpha, 1)$, $C_n = \frac{p_s}{\kappa} Z(\beta_n^{(D)}, \alpha, 0)$, $D_n = 1 + B_n - C_n$, $E_n = C_n + A_n(1 + B_n - C_n)$, and $J_n = \mu_n \gamma_n^{(Q)}$.

IV. JOINT OPTIMIZATION OF SERVICE CACHING DISTRIBUTION AND COMPUTING RESOURCE ALLOCATION

In this section, we formulate the SSP maximization problem, and then, by using the parallel successive convex approximation (SCA), we propose an iterative algorithm to obtain the stationary point of the problem.

A. Problem Formulation

The SSP is affected by the random service caching and the computing capability of the EC server. Therefore, we maximize the SSP by optimizing the service caching distribution \mathbf{a} and the computing resource allocation \mathbf{b} as formulated below.

Problem 1 (SSP maximization):

$$\begin{aligned} \max_{\mathbf{a}, \mathbf{b}} \quad & \tilde{\mathcal{P}}_k(\mathbf{a}, \mathbf{b}) \\ \text{s.t.} \quad & (2), (3), (7), (8), (15), \end{aligned}$$

where $k \in \{m, d\}$ and $\tilde{\mathcal{P}}_k(\mathbf{a}, \mathbf{b})$ is in (22) and (23). Here, T_n is the service caching probability, which is defined in (4). Note that since (2) and (3) imply (5) and (6), we can ignore (5) and (6).

Then, we obtain an equivalent problem of Problem 1 by including inequality constraints in (15) implicitly in the objective function using the logarithmic barrier term as follows.

Problem 2 (Equivalent problem of Problem 1):

$$\begin{aligned} \max_{\mathbf{a}, \mathbf{b}} \quad & \tilde{\mathcal{P}}_k(\mathbf{a}, \mathbf{b}) + \frac{1}{\omega} \phi(\mathbf{a}, \mathbf{b}) \\ \text{s.t.} \quad & (2), (3), (7), (8), \end{aligned}$$

where $\omega \gg 0$ is a large positive value and $\phi(\mathbf{a}, \mathbf{b}) = \sum_{n \in \mathcal{N}} \sum_{j \in \mathcal{J}_n} \log(b_{n,j} \mu_n - \lambda_n(\mathbf{a}))$. Note that Problem 2 becomes infeasible if the queue stability condition in (15) is not satisfied (i.e., $b_{n,j} \mu_n < \lambda_n(\mathbf{a})$) since the logarithm of a negative value is not defined.

In the RT case (i.e., $k = m$), the objective function in Problem 2 is marginally concave w.r.t. \mathbf{b} , but not jointly concave w.r.t. \mathbf{a} and \mathbf{b} . The constraints in Problem 2 are all linear. Therefore, Problem 2 for the RT case is a nonconvex problem. On the other hand, in the DT case (i.e., $k = d$), Problem 2 is also a nonconvex problem since the objective function is not jointly concave w.r.t. \mathbf{a} and \mathbf{b} and the constraints are linear functions.

B. Optimal Solution

In general, it is hard to obtain a globally optimal solution for a nonconvex problem with an effective and efficient method. A classic goal for dealing with a nonconvex problem is to obtain a stationary point that satisfies the Karush-Kuhn-Tucker (KKT) conditions. Hence, we propose an iterative algorithm to obtain the stationary point of Problem 2 by using the parallel SCA [18]. Specifically, we divide the variables (\mathbf{a} , \mathbf{b}) into one block for \mathbf{a} and J blocks for $\mathbf{b}_j \triangleq (b_{n,j})_{n \in \mathcal{N}_j}$, since the constraints are block separable. At each iteration, we solve one problem w.r.t. \mathbf{a} and J problems w.r.t. $\mathbf{b}_j, j \in \mathcal{J}$, in a parallel manner.

- For \mathbf{a} , we solve the approximate convex problem for both the RT and the DT cases.

Problem 3 (Approximate Problem 2 for \mathbf{a} at iteration $r + 1$):

$$\max_{\mathbf{a}} \quad \tilde{\mathcal{F}}_{\mathbf{a},k}(\mathbf{a}, \mathbf{a}_k^{(r)}, \mathbf{b}_k^{(r)}), \quad \text{s.t. (2), (3), } k \in \{m, d\},$$

where $\mathbf{a}_k^{(r)}$ and $\mathbf{b}_k^{(r)}$ are the service caching distribution, and computing resource allocation at iteration r , and $\tilde{\mathcal{F}}_{\mathbf{a},k}(\mathbf{a}, \mathbf{a}_k^{(r)}, \mathbf{b}_k^{(r)})$ is the approximation of the objective function in Problem 2 for \mathbf{a} , which is obtained in (25) later.

- For $\mathbf{b}_j, j \in \mathcal{J}$, the objective function in Problem 2 is separated into J sub-objective functions, i.e.,

$$\begin{aligned} \mathcal{F}_{\mathbf{b}_j,k}(\mathbf{b}_j, \mathbf{a}_k^{(r)}) = & \sum_{n \in \mathcal{N}_j} p_n P_n^{(U)}(\mathbf{a}) P_n^{(D)}(\mathbf{a}) \tilde{P}_{n,i,k}^{(Q)}(\mathbf{a}, \mathbf{b}) \\ & + \frac{\log(b_{n,j} \mu_n - \lambda_n(\mathbf{a}_k^{(r)}))}{\omega}, \end{aligned} \quad (24)$$

for $k \in \{m, d\}$. Since $\mathcal{F}_{\mathbf{b}_j,k}(\mathbf{b}_j, \mathbf{a}_k^{(r)})$ is negative semidefinite, the objective function in (24) is a concave function with respect to \mathbf{b}_j .

Then, we solve the convex problem for the RT case.

Problem 4 (Problem 2 for \mathbf{b}_j at iteration $r + 1$ in the RT case):

$$\max_{\mathbf{b}_j} \quad \mathcal{F}_{\mathbf{b}_j,m}(\mathbf{b}_j, \mathbf{a}_m^{(r)}), \quad \text{s.t. (7), (8).}$$

On the other hand, we solve the approximate convex problem for the DT case.

Problem 5 (Approximate Problem 2 for \mathbf{b}_j at iteration $r + 1$ in the DT case):

$$\max_{\mathbf{b}_j} \quad \tilde{\mathcal{F}}_{\mathbf{b}_j,d}(\mathbf{b}_j, \mathbf{a}_d^{(r)}, \mathbf{b}_d^{(r)}), \quad \text{s.t. (7), (8),}$$

where $\tilde{\mathcal{F}}_{\mathbf{b}_j,d}(\mathbf{b}_j, \mathbf{a}_d^{(r)}, \mathbf{b}_d^{(r)})$ is the approximation of $\mathcal{F}_{\mathbf{b}_j,d}(\mathbf{b}_j, \mathbf{a}_d^{(r)})$ for \mathbf{b}_j , which is obtained in (33) later.

Then, using the optimal solutions of Problem 3, 4 and 5, we update the service caching distribution \mathbf{a} and the computing resource allocation \mathbf{b} , respectively, in a parallel manner.

1) *Optimal Service Caching Distribution*: First, we choose the approximation function of $\tilde{\mathcal{P}}_k(\mathbf{a}, \mathbf{b}) - \frac{1}{\omega}\phi(\mathbf{a}, \mathbf{b})$, $k \in \{m, d\}$ by taking the second order Taylor expansion for \mathbf{a} , given by

$$\tilde{\mathcal{F}}_{\mathbf{a},k}(\mathbf{a}, \mathbf{a}_k^{(r)}, \mathbf{b}_k^{(r)}) \triangleq -\mathbf{a}^T \mathbf{a} + \left(2\mathbf{a}_k^{(r)} + \nabla_{\mathbf{a}} \left(\tilde{\mathcal{P}}_k(\mathbf{a}, \mathbf{b}) - \frac{1}{\omega}\phi(\mathbf{a}, \mathbf{b}) \right) \Big|_{\mathbf{a}=\mathbf{a}_k^{(r)}} \right)^T \mathbf{a}, \quad (25)$$

where \mathbf{x}^T is the transpose of \mathbf{x} . Note that the SCA algorithm obtains the stationary point of Problem 2 to solve the convex problem 3 using the approximated objective function in (25). Therefore, the optimal solution of Problem 3 is given by

$$\bar{\mathbf{a}}_k^{(r+1)} \triangleq \operatorname{argmax}_{\mathbf{a} \in \mathcal{X}_a} \tilde{\mathcal{F}}_{\mathbf{a},k}(\mathbf{a}, \mathbf{a}_k^{(r)}, \mathbf{b}_k^{(r)}), \quad k \in \{m, d\}, \quad (26)$$

where \mathcal{X}_a is the feasible convex set of constraints (2) and (3). Since Problem 3 is the convex optimization problem, we can obtain $\bar{\mathbf{a}}_k^{(r+1)}$, $k \in \{m, d\}$ by using standard convex optimization techniques such as the interior point method [34]. Finally, we update $\mathbf{a}_k^{(r)}$ at iteration $r+1$ by

$$\mathbf{a}_k^{(r+1)} = \mathbf{a}_k^{(r)} + \alpha^{(r+1)} \left(\bar{\mathbf{a}}_k^{(r+1)} - \mathbf{a}_k^{(r)} \right), \quad k \in \{m, d\}, \quad (27)$$

where $\alpha^{(r+1)}$ is a positive diminishing step size that satisfies

$$\alpha^{(r+1)} > 0, \lim_{r \rightarrow \infty} \alpha^{(r+1)} = 0, \quad \sum_{r=1}^{\infty} \alpha^{(r+1)} = \infty, \lim_{r \rightarrow \infty} \left(\alpha^{(r+1)} \right)^2 < \infty. \quad (28)$$

2) *Optimal Computing Resource Allocation*: In the RT case, the optimal solution of Problem 4 is given by

$$\bar{\mathbf{b}}_{j,m}^{(r+1)} \triangleq \operatorname{argmax}_{\mathbf{b}_j \in \mathcal{X}_b} \mathcal{F}_{\mathbf{b}_j,m}(\mathbf{b}_j, \mathbf{a}_m^{(r)}), \quad (29)$$

where \mathcal{X}_b is the feasible convex set of constraints (7) and (8). Since Problem 4 is convex and the strong duality holds, we can obtain $\bar{\mathbf{b}}_{j,m}^{(r+1)}$ using KKT conditions.

Lemma 1 (Optimal Solution of Problem 4):

$$\bar{b}_{n,j,m}^{(r+1)} = \max \left(G_{n,j}^{-1} \left(\eta_j^{*(r+1)} \right), 0 \right), \quad n \in \mathcal{N}, j \in \mathcal{J}_n, \quad (30)$$

where $\eta_j^{*(r+1)}$ satisfies $\sum_{n \in \mathcal{N}_j} \max \left(G_{n,j}^{-1} \left(\eta_j^{*(r+1)} \right), 0 \right) = 1$ and $G^{-1}(\cdot)$ is the inverse function of $G(\cdot)$, which is given by

$$G_{n,j}(b_{n,j}) = \frac{J_n p_n a_{j,m}^{(r)} T_{n,m}^{(r)} e^{\lambda_{n,m}^{(r)} \gamma_n^{(0)} - b_{n,j} J_n}}{D_n \left(T_{n,m}^{(r)} \right)^2 + E_n T_{n,m}^{(r)} + A_n^2} + \frac{\mu_n}{\omega} e^{\phi_{n,j}(\mathbf{a}_m^{(r)}, b_{n,j})}, \quad (31)$$

where $\phi_{n,j}(\mathbf{a}_m^{(r)}, b_{n,j}) = \log \left(b_{n,j} \mu_n - \lambda_n \left(\mathbf{a}_m^{(r)} \right) \right)$.

Proof: See Appendix A. ■

In (31), $G(b_{n,j})$ is a decreasing function since its derivative is negative. As $G(\bar{b}_{n,j,m}^{(r+1)})$ is monotonically decreasing with $\bar{b}_{n,j,m}^{(r+1)}$, $G^{-1}(\eta_j^{*(r+1)})$ is also monotonically decreasing with

Algorithm 1 Obtaining A Stationary Point of Problem 2

- 1: Initialize $\mathbf{a}^{(0)}, \mathbf{b}^{(0)}$ which are feasible solution of Problem 2, and set $r = 1$.
 - 2: **while** $\left\| \nabla \left(\tilde{\mathcal{P}}_k(\mathbf{a}, \mathbf{b}) - \frac{1}{\omega}\phi(\mathbf{a}, \mathbf{b}) \right) \right\|^2 \geq \tau$, $k \in \{m, d\}$ **do**
 - 3: Obtain $\bar{\mathbf{a}}_k^{(r+1)}$, $k \in \{m, d\}$ by solving Problem 3 using the interior point method.
 - 4: Update $\mathbf{a}_k^{(r)}$, $k \in \{m, d\}$ according to (27).
 - 5: **for** $j \in \mathcal{J}$ **do**
 - 6: **if** $k = m$ **then**
 - 7: Obtain $\bar{\mathbf{b}}_{j,m}^{(r+1)}$ according to (30).
 - 8: Update $\mathbf{b}_{j,m}^{(r)}$ according to (32).
 - 9: **else**
 - 10: Obtain $\bar{\mathbf{b}}_{j,d}^{(r+1)}$ by solving Problem 5 using the interior point method.
 - 11: Update $\mathbf{b}_{j,d}^{(r)}$ according to (35).
 - 12: Set $r = r + 1$.
-

$\eta_j^{*(r+1)}$. Therefore, $\eta_j^{*(r+1)}$ and $\bar{b}_{n,j,m}^{(r+1)}$ can be easily obtained by using the bisection method. Then, we update $\mathbf{b}_{j,m}^{(r)}$ at iteration $r+1$ by

$$\mathbf{b}_{j,m}^{(r+1)} = \mathbf{b}_{j,m}^{(r)} + \alpha^{(r+1)} \left(\bar{\mathbf{b}}_{j,m}^{(r+1)} - \mathbf{b}_{j,m}^{(r)} \right), \quad j \in \mathcal{J}. \quad (32)$$

In the DT case, we choose the approximation function of $\mathcal{F}_{\mathbf{b}_j,d}(\mathbf{b}_j, \mathbf{a}_d^{(r)})$ by taking the second order Taylor expansion for \mathbf{b}_j , which is given by

$$\begin{aligned} \tilde{\mathcal{F}}_{\mathbf{b}_j,d}(\mathbf{b}_j, \mathbf{a}_d^{(r)}, \mathbf{b}_d^{(r)}) \\ \triangleq -\mathbf{b}_j^T \mathbf{b}_j + \left(2\mathbf{b}_{j,d}^{(r)} + \nabla_{\mathbf{b}_j} \mathcal{F}_{\mathbf{b}_j,d}(\mathbf{b}_j, \mathbf{a}_d^{(r)}) \Big|_{\mathbf{b}_{j,d}=\mathbf{b}_{j,d}^{(r)}} \right)^T \mathbf{b}_j, \end{aligned} \quad j \in \mathcal{J}. \quad (33)$$

Then, the optimal solution of Problem 5 is given by

$$\bar{\mathbf{b}}_{j,d}^{(r+1)} \triangleq \operatorname{argmax}_{\mathbf{b}_j \in \mathcal{X}_b} \tilde{\mathcal{F}}_{\mathbf{b}_j,d}(\mathbf{b}_j, \mathbf{a}_d^{(r)}, \mathbf{b}_d^{(r)}). \quad (34)$$

Since Problem 5 is the convex optimization problem, we can obtain $\bar{\mathbf{b}}_{j,d}^{(r+1)}$ by using the interior point method [34]. Then, we update $\mathbf{b}_{j,d}^{(r)}$ at iteration $r+1$ by

$$\mathbf{b}_{j,d}^{(r+1)} = \mathbf{b}_{j,d}^{(r)} + \alpha^{(r+1)} \left(\bar{\mathbf{b}}_{j,d}^{(r+1)} - \mathbf{b}_{j,d}^{(r)} \right), \quad j \in \mathcal{J}. \quad (35)$$

Finally, the details of the proposed iterative algorithm are summarized in Algorithm 1. Based on Theorem 1 in [18], we can derive the following result in Lemma 2.

Lemma 2 (Convergence of Algorithm 1): When the step size $\alpha^{(r+1)}$ satisfies the conditions in (28), $\lim_{r \rightarrow \infty} \left(\mathbf{a}_k^{(r)}, \mathbf{b}_k^{(r)} \right)$, $k \in \{m, d\}$ are always stationary points of Problem 1.

Proof: First, it is obvious that $\tilde{\mathcal{F}}_{\mathbf{a},k}(\mathbf{a}, \mathbf{a}_k^{(r)}, \mathbf{b}_k^{(r)})$, $k \in \{m, d\}$, $\mathcal{F}_{\mathbf{b}_j,m}(\mathbf{b}_j, \mathbf{a}_m^{(r)})$, and $\tilde{\mathcal{F}}_{\mathbf{b}_j,d}(\mathbf{b}_j, \mathbf{a}_d^{(r)}, \mathbf{b}_d^{(r)})$ are differentiable for any given \mathbf{a} and \mathbf{b} , respectively. Moreover, the Hessian of $\tilde{\mathcal{F}}_{\mathbf{a},k}(\mathbf{a}, \mathbf{a}_k^{(r)}, \mathbf{b}_k^{(r)})$ and $\tilde{\mathcal{F}}_{\mathbf{b}_j,d}(\mathbf{b}_j, \mathbf{a}_d^{(r)}, \mathbf{b}_d^{(r)})$ is always negative. Second, in (25), the gradient of $\tilde{\mathcal{F}}_{\mathbf{a},k}(\mathbf{a}, \mathbf{a}_k^{(r)}, \mathbf{b}_k^{(r)})$ w.r.t. \mathbf{a} is the same as the gradient

of objective function in Problem 2 w.r.t. \mathbf{a} . Moreover, in (33), the gradient of $\tilde{\mathcal{F}}_{\mathbf{b}_j, \mathbf{d}}(\mathbf{b}_j, \mathbf{a}_d^{(r)}, \mathbf{b}_d^{(r)})$ w.r.t. \mathbf{b}_j is the same as that of objective function in Problem 2 w.r.t. \mathbf{b}_j . Finally, $\tilde{\mathcal{F}}_{\mathbf{a}, k}(\mathbf{a}, \mathbf{a}_k^{(r)}, \mathbf{b}_k^{(r)})$, $\mathcal{F}_{\mathbf{b}_j, \mathbf{m}}(\mathbf{b}_j, \mathbf{a}_m^{(r)})$, and $\tilde{\mathcal{F}}_{\mathbf{b}_j, \mathbf{d}}(\mathbf{b}_j, \mathbf{a}_d^{(r)}, \mathbf{b}_d^{(r)})$ are smooth functions on the constraints in (2),(3),(7), and (8). Therefore, using Theorem 1 in [18], Lemma 2 is obtained. ■

It is known that for a given step size and an initial point, the number of iterations in parallel SCA is always constant [18]. Thus, the complexity order of Algorithm 1 is identical to that of each iteration in it. At each iteration, we solve one problem w.r.t. \mathbf{a} and J problems w.r.t. $\mathbf{b}_j, j \in \mathcal{J}$. In the case of solving the problem w.r.t. \mathbf{a} using the interior point method, the computational complexity is $\mathcal{O}(N^{7K/2})$. In the case of solving the problem w.r.t. $\mathbf{b}_j, j \in \mathcal{J}$, we consider two cases for the computational complexity. In the RT case, the bisection method is used, so the computation complexity is $\mathcal{O}(N^K K^3)$. On the other hand, in the DT case, the interior point method is used, so the computational complexity is $\mathcal{O}(N^K K^{7/2})$. Therefore, the overall complexity of Algorithm 1 is $\mathcal{O}(N^{7K/2})$ regardless of the service time case.

Note that the service popularity, i.e., p_n , is the average value for certain time period and region. This means p_n can vary over time and space. For that case, the proposed algorithm can be performed again to find the optimal solution for the changed environment⁵.

V. ASYMPTOTIC SOLUTION FOR JOINT OPTIMIZATION OF SERVICE CACHING DISTRIBUTION AND COMPUTING RESOURCE ALLOCATION

In Problem 2, there exist J optimization variables for \mathbf{a} and KJ optimization variables for \mathbf{b} . In addition, despite the use of parallel SCA, obtaining the stationary point of Problem 2 requires the high complex algorithm, especially for a large N . Therefore, in this section, we consider an asymptotic version of Problem 2 for a special case that the computing capability of the EC server is infinity, i.e., infinite computing capability case. Then, we develop an iterative algorithm to obtain an asymptotically optimal solution for this case. Finally, using the asymptotically optimal solution, we develop a low complex algorithm to obtain a near-optimal solution of Problem 2 in high computing capability region.

From equation (22) and (23), we can see that the physical layer parameters (i.e., $\alpha, W, \lambda_u, \lambda_{bs}, F_{bs}$) and the design parameters (\mathbf{a}, \mathbf{b}) jointly affect the SSP. Moreover, the impacts of physical layer parameters and the design parameters on $\tilde{\mathcal{P}}_k(\mathbf{a}, \mathbf{b})$ are coupled in a complex manner. Therefore, to make a low complex algorithm to maximize the SSP, we need to simplify the SSP to have decoupled effects from the physical layer and the design parameters. For this, we analyze the asymptotic SSP in the infinite computing capability case. From (22) and (23), it is obvious that the SSP increases with the computing capability F_{bs} , so we have the following corollary.

⁵The frequency of updating the service caching and computing resource allocation can be the networks management issue.

Corollary 1 (Asymptotic Performance): When $F_{bs} \rightarrow \infty$, for $k = \{m, d\}$, we have

$$\begin{aligned} \mathcal{P}_\infty(\mathbf{a}) &\triangleq \lim_{F_{bs} \rightarrow \infty} \tilde{\mathcal{P}}_k(\mathbf{a}, \mathbf{b}) \\ &= \sum_{n \in \mathcal{N}} \frac{p_n \left(\sum_{j \in \mathcal{J}_n} a_j \right)^2}{D_n \left(\sum_{j \in \mathcal{J}_n} a_i \right)^2 + E_n \left(\sum_{j \in \mathcal{J}_n} a_j \right) + A_n C_n}. \end{aligned} \quad (36)$$

Proof: When $F_{bs} \rightarrow \infty$, we have $J_n = \frac{F_{bs}}{f_n} \gamma_n^{(Q)} \rightarrow \infty$. Thus, for $j \in \mathcal{J}$, $n \in \mathcal{N}_j$, we have

$$\exp\left(-b_{n,j} J_n + \lambda_n \gamma_n^{(Q)}\right) \rightarrow 0, \quad (37)$$

$$\begin{aligned} \sum_{k=0}^{\lfloor J_n \rfloor} \frac{\lambda_n^k \left(\frac{k}{b_{n,j} \mu_n} - \gamma_n^{(Q)} \right)^k e^{\lambda_n \left(\gamma_n^{(Q)} - \frac{k}{b_{n,j} \mu_n} \right) - \delta(k - b_{n,j} J_n)}}{k! \left(1 + e^{-\delta(k - b_{n,j} J_n)} \right)} \\ \rightarrow 1. \end{aligned} \quad (38)$$

Therefore, by substituting (37) and (38) into (22) and (23), respectively, we obtain $\mathcal{P}_\infty(\mathbf{a})$, which is given by (36). ■

From Corollary 1, we can see that in infinite computing capability case, some physical layer parameters such as λ_u and λ_{bs} , and the design parameter \mathbf{b} do not affect the SSP. Moreover, the impacts of the physical layer parameter p_n and the design parameter \mathbf{a} on (36) are more clearly shown. In addition, the asymptotic SSP in (36) has a simpler form than $\tilde{\mathcal{P}}_m(\mathbf{a}, \mathbf{b})$ in (22) and $\tilde{\mathcal{P}}_d(\mathbf{a}, \mathbf{b})$ in (23).

Now, we maximize the asymptotic SSP in (36) by optimizing the service caching distribution. Note that the stability condition of the queue in (15) is always satisfied due to the high computing capability. Therefore, we have the following asymptotic optimization problem.

Problem 6 (Asymptotic SSP maximization):

$$\begin{aligned} \bar{\mathbf{a}}_\infty &\triangleq \arg \max_{\mathbf{a}} \mathcal{P}_\infty(\mathbf{a}) \\ &\text{s.t.} \quad (2), (3). \end{aligned}$$

Note that $\bar{\mathbf{a}}_\infty$ is an asymptotically optimal solution of Problem 1. In Problem 6, by replacing $\mathcal{P}_\infty(\mathbf{a})$ with $\mathcal{P}_\infty(\mathbf{T})$, we have the following optimization problem.

Problem 7 (Equivalent problem of Problem 6):

$$\begin{aligned} \bar{\mathbf{T}}_\infty &\triangleq \arg \max_{\mathbf{T}} \mathcal{P}_\infty(\mathbf{T}) \\ &\text{s.t.} \quad (5), (6). \end{aligned}$$

We can show that Problem 7 is equivalent to Problem 6.

Lemma 3 (Equivalence of Problem 6 and 7): The solutions of Problem 6 and Problem 7 satisfy

$$\sum_{j \in \mathcal{J}_n} \bar{a}_{j,\infty} = \bar{T}_{n,\infty}, \quad n \in \mathcal{N}, \quad \mathcal{P}_\infty(\bar{\mathbf{a}}_\infty) = \mathcal{P}_\infty(\bar{\mathbf{T}}_\infty). \quad (39)$$

Proof: For given $\bar{\mathbf{a}}_\infty$, we can easily obtain $\bar{\mathbf{T}}_\infty$ which satisfies the conditions in (5) and (6). On the other hand, for given $\bar{\mathbf{T}}_\infty$, we can obtain $\bar{\mathbf{a}}_\infty$ which satisfies the conditions in (2) and (3) by using the method in Fig. 1. of [35]. Moreover,

due to the communication performance is affected only by whether the BS has the service software n or not, for given any $\bar{\mathbf{a}}_\infty$ and $\bar{\mathbf{T}}_\infty$, the optimal value of Problem 6 and Problem 7 are the same, i.e., $\mathcal{P}_\infty(\bar{\mathbf{a}}_\infty) = \mathcal{P}_\infty(\bar{\mathbf{T}}_\infty)$. ■

In Problem 7, the objective function is convex w.r.t. \mathbf{T} and all constraints are affine. Since Problem 7 is a problem that maximizes the convex function, it is a nonconvex problem. Specifically, Problem 7 is a special case of the difference of convex function (DC) programming problem.

A. Asymptotic Optimal Solution For Infinite Computing Capability Case

In this subsection, we provide an asymptotically optimal solution of Problem 7 for infinite computing capability case. We propose an iterative algorithm to obtain the stationary point of Problem 7 using the concave-convex procedure (CCCP) [36]. Specifically, at each iteration, we choose the approximation function of $\mathcal{P}_\infty(\mathbf{T})$ by taking the linear approximation, given by

$$\begin{aligned} \tilde{\mathcal{P}}_\infty(\mathbf{T}, \mathbf{T}^{(r)}) &\triangleq (\nabla_{\mathbf{T}} \mathcal{P}_\infty(\mathbf{T})|_{\mathbf{T}=\mathbf{T}^{(r)}})^T (\mathbf{T} - \mathbf{T}^{(r)}) \\ &\quad + \mathcal{P}_\infty(\mathbf{T}^{(r)}), \end{aligned} \quad (40)$$

where $\mathbf{T}^{(r)}$ is the service probability distribution at iteration r . Then, we update the service probability distribution $\mathbf{T}^{(r)}$ at iteration $r+1$ by

$$\mathbf{T}^{(r+1)} = \operatorname{argmax}_{\mathbf{T} \in \mathcal{X}_t} \tilde{\mathcal{P}}_\infty(\mathbf{T}, \mathbf{T}^{(r)}), \quad (41)$$

where \mathcal{X}_t is the feasible convex set of constraints (5) and (6). Based on Theorem 4 in [37], we can show the following result in Lemma 4.

Lemma 4: By using the update rule in (41), the convergence point $\lim_{r \rightarrow \infty} \mathbf{T}^{(r)}$ is always a stationary point of Problem 7.

Proof: We can see that the objective function $\mathcal{P}_\infty(\mathbf{T})$ in Problem 7 is a differentiable convex function. Moreover, we can see that the gradient of $\mathcal{P}_\infty(\mathbf{T})$ in Problem 7 is continuous. By using the linear approximation function, we can always find an optimal solution $\mathbf{T}^{(r)}$ at each iteration, which satisfies the condition in (41). Finally, the set of optimal solutions is compact on the constraints in (5) and (6). Therefore, using Theorem 4 in [37], Lemma 4 is obtained. ■

It is known that for a given step size and an initial point, the number of iterations for CCCP is constant [36]. Thus, the computational complexity order of Problem 7 is identical to that of each iteration in it. At each iteration, we solve one approximate convex problem w.r.t. \mathbf{T} , so the computational complexity of solving the problem w.r.t. \mathbf{T} using the interior point method is $\mathcal{O}(N^{7/2})$. Therefore, the overall complexity of solving Problem 7 is $\mathcal{O}(N^{7/2})$.

B. Near-Optimal Solution In High Computing Capability Region

In this subsection, we consider the near-optimal solution in high computing capability region for given asymptotically optimal solution of the infinite computing capability case. Specifically, for given the asymptotically optimal solution of

the service probability \mathbf{T}^* in (39), we formulate the SSP maximization problem, and develop an iterative algorithm with low computational complexity to obtain a near-optimal solution in the high computing capability region.

First of all, for given \mathbf{T}^* , we now maximize the SSP by optimizing the service caching distribution \mathbf{a} and the computing resource allocation \mathbf{b} in the high computing capability region.

Problem 8 (SSP maximization for given \mathbf{T}^):*

$$\begin{aligned} \max_{\mathbf{a}, \mathbf{b}} \quad & \mathcal{P}_k(\mathbf{a}, \mathbf{b}, \mathbf{T}^*) \\ \text{s.t.} \quad & (2), (39), (7), (8), (15), \end{aligned}$$

where $k \in \{m, d\}$. Here, $\mathcal{P}_m(\mathbf{a}, \mathbf{b}, \mathbf{T}^*)$ and $\mathcal{P}_d(\mathbf{a}, \mathbf{b}, \mathbf{T}^*)$ are obtained by substituting \mathbf{T}^* into \mathbf{T} in (22) and (23), respectively.

In the RT case (i.e., $k = m$), the objective function in Problem 8 is a jointly concave function w.r.t. \mathbf{a} and \mathbf{b} . On the other hand, in the DT case (i.e., $k = d$), the objective function in Problem 8 is an affine function w.r.t. \mathbf{a} but not jointly concave w.r.t. \mathbf{a} and \mathbf{b} . Therefore, for given \mathbf{T}^* , Problem 8 is a nonconvex problem.

To obtain the stationary point of Problem 8 that satisfies the KKT condition, we develop an algorithm with low complexity for each service time case.

1) Random Service Time Case: In the RT case, we divide Problem 8 into one master problem w.r.t. \mathbf{a} and J subproblems w.r.t. \mathbf{b}_j by noting that the constraints on $J+1$ problems are separable. We first obtain an optimal solution of J subproblems w.r.t. \mathbf{b}_j . Then, for a given optimal solution of the subproblems w.r.t. \mathbf{b}_j , we obtain the optimal solution of the master problem w.r.t. \mathbf{a} . The details are further illustrated below. The master problem is formulated as follows.

Problem 9 (Master problem - service caching distribution):

$$\begin{aligned} \max_{\mathbf{a}} \quad & \sum_{n \in \mathcal{N}} \mathcal{P}_\infty(\mathbf{T}^*) + \sum_{j \in \mathcal{J}} \bar{\mathcal{H}}_{j,m}(\mathbf{T}^*) a_j \\ \text{s.t.} \quad & (2), (39), \end{aligned}$$

where $\bar{\mathcal{H}}_{j,m}(\mathbf{T}^*)$ is given by the following subproblem.

Problem 10 (Subproblem - computing resource allocation):

$$\begin{aligned} \bar{\mathcal{H}}_{j,m}(\mathbf{T}^*) &\triangleq \max_{\mathbf{b}_j} \mathcal{H}_{j,m}(\mathbf{b}_j, \mathbf{T}^*) \\ \text{s.t.} \quad & (7), (8), (15), \end{aligned}$$

where $\mathcal{H}_{j,m}(\mathbf{b}_j, \mathbf{T}^*)$ is given by

$$\begin{aligned} \mathcal{H}_{j,m}(\mathbf{b}_j, \mathbf{T}^*) &= - \sum_{n \in \mathcal{N}_j} \frac{P_n}{T_n^*} P_n^{(U)}(\mathbf{T}^*) P_n^{(D)}(\mathbf{T}^*) \\ &\quad \times e^{-(b_{n,j} \mu_n - \lambda_n^*) \gamma_n^{(Q)}}, \end{aligned} \quad (42)$$

where $\lambda_n^* = \frac{T_n^* + C_n}{T_n^* + A_n}$.

Since Problem 10 is convex and the strong duality holds, we obtain the optimal solution $\mathbf{b}_{j,m}$ of Problem 10 by using KKT conditions.

Lemma 5 (Optimal Solution of Problem 10):

$$\bar{b}_{n,j,m} = \frac{1}{J_n} \left\{ \log \left(\frac{J_n p_n (T_n^*)^2}{\hat{\zeta}_j^* (D_n (T_n^*)^2 + E_n T_n^* + A_n^2)} \right) + \lambda_n^* \gamma_n^{(Q)} \right\}, \quad n \in \mathcal{N}_j, j \in \mathcal{J}, \quad (43)$$

where $\hat{\zeta}_j^*$ is the Lagrange multiplier which satisfies the constraint in (8).

Proof: See Appendix B. \blacksquare

Next, we solve Problem 9. From Lemma 5, for given $\bar{\mathbf{b}}_m$, Problem 9 becomes:

Problem 11 (Service caching distribution for given $\bar{\mathbf{b}}_m$):

$$\begin{aligned} \max_{\mathbf{a}} \quad & \sum_{n \in \mathcal{N}} \mathcal{P}_{\infty}(\mathbf{T}^*) - \sum_{j \in \mathcal{J}} \sum_{n \in \mathcal{N}_j} \frac{\hat{\zeta}_j^*}{J_n} a_j \\ \text{s.t.} \quad & (2), (39). \end{aligned}$$

In Problem 11, the objective function and all constraints are affine functions, so it is a linear programming (LP) problem. To reduce the complexity, we formulate a dual problem of Problem 11 with the dual variable $\mathbf{w} = (w_n)_{n \in \mathcal{N}}$. When $\bar{\mathbf{a}}_m$ is the optimal solution of Problem 11, we have

$$\sum_{j \in \mathcal{J}} \sum_{n \in \mathcal{N}_j} -\frac{\hat{\zeta}_j^*}{J_n} \bar{a}_{j,m} = \sum_{n \in \mathcal{N}} \bar{w}_n T_n^*, \quad (44)$$

where $\bar{\mathbf{w}}$ is the optimal solution of the dual problem, which is formulated as follows.

Problem 12 (Dual problem of Problem 11):

$$\begin{aligned} \bar{\mathbf{w}} \triangleq \arg \max_{\mathbf{w}} \quad & \sum_{n \in \mathcal{N}} w_n T_n^* \\ \text{s.t.} \quad & \sum_{n \in \mathcal{N}_j} w_n \leq \sum_{n \in \mathcal{N}_j} -\frac{\hat{\zeta}_j^*}{J_n}, \quad j \in \mathcal{J}. \end{aligned}$$

Since Problem 12 is a convex problem, we can easily obtain an optimal solution $\bar{\mathbf{w}}$ by using the interior point method [34]. Then, from (44), for given $\bar{\mathbf{w}}$, we can easily obtain the optimal solution $\bar{\mathbf{a}}_m$. Finally, we can obtain the near-optimal solution $\bar{\mathbf{a}}_m$ and $\bar{\mathbf{b}}_m$ of Problem 8, as summarized in Algorithm 2.

Now, we consider the computational complexity. In the RT case, since the optimal solution of Problem 10 is expressed as the closed form in (43), the computational complexity of solving the problem w.r.t. \mathbf{b}_j is $\mathcal{O}(K)$. Hence, the computational complexity of solving the problem w.r.t. \mathbf{b} is $\mathcal{O}(N^K K)$, where N^K is the number of service combinations. In Problem 12, the interior point method is used, so the total computational complexity is $\mathcal{O}(N^{2+3K/2})$. We can argue that the computational complexity in obtaining the near-optimal solution of Problem 8 is lower than that of obtaining the optimal solution of Problem 2, which is $\mathcal{O}(N^{7K/2})$.

2) *Deterministic Service Time Case:* In the DT case, we propose an iterative algorithm to obtain the stationary point of Problem 8 by using parallel SCA. Specifically, we divide the variables (\mathbf{a}, \mathbf{b}) into one block for \mathbf{a} and J blocks for \mathbf{b}_j

since the constraints are block separable. At each iteration, we first solve one convex problem w.r.t. \mathbf{a} .

Problem 13 (Approximate Problem 8 for \mathbf{a} at iteration $r+1$):

$$\begin{aligned} \max_{\mathbf{a}} \quad & \mathcal{P}_d(\mathbf{a}, \hat{\mathbf{b}}_d^{(r)}, \mathbf{T}^*) \\ \text{s.t.} \quad & (2), (39). \end{aligned}$$

where $\hat{\mathbf{b}}_d^{(r)}$ is the computing resource allocation for given \mathbf{T}^* at iteration r , which is obtained in Problem 15 later. The objective function of Problem 13 is an affine function w.r.t. \mathbf{a} and all constraints are affine functions, so Problem 13 is a LP problem. To reduce the computational complexity, we formulate the dual problem of Problem 13 with dual variables $\mathbf{v} = (v_n)_{n \in \mathcal{N}}$. Specifically, when $\bar{\mathbf{a}}_{d, \mathbf{T}^*}^{(r+1)}$ is the optimal solution of Problem 13, we have

$$\mathcal{P}_d(\bar{\mathbf{a}}, \hat{\mathbf{b}}_d^{(r)}, \mathbf{T}^*) = \sum_{n \in \mathcal{N}} \bar{v}_n^{(r+1)} T_n^*. \quad (45)$$

where $\bar{\mathbf{v}}^{(r+1)}$ is the optimal solution of dual problem, which is formulated as follows.

Problem 14 (Dual problem of Problem 13):

$$\begin{aligned} \bar{\mathbf{v}}^{(r+1)} \triangleq \max_{\mathbf{v}} \quad & \sum_{n \in \mathcal{N}} v_n T_n^* \\ \text{s.t.} \quad & \sum_{n \in \mathcal{N}_j} v_n \leq G_j(\hat{\mathbf{b}}_d^{(r)}, \mathbf{T}^*), \quad j \in \mathcal{J}, \end{aligned}$$

where $G_j(\hat{\mathbf{b}}_d^{(r)}, \mathbf{T}^*)$, $j \in \mathcal{J}$ is given by

$$\begin{aligned} G_j(\hat{\mathbf{b}}_d^{(r)}, \mathbf{T}^*) = & \sum_{n \in \mathcal{N}_j} \frac{p_n}{T_n^*} P_n^{(U)}(\mathbf{T}^*) P_n^{(D)}(\mathbf{T}^*) \left(1 - \frac{\lambda_n^*}{\hat{b}_{n,j,d}^{(r)} \mu_n} \right) \\ & \times \sum_{k=0}^{\lfloor J_n \rfloor} \frac{(\lambda_n^*)^k \left(\frac{k}{\hat{b}_{n,j,d}^{(r)} \mu_n} - \gamma_n^{(Q)} \right)^k e^{\lambda_n^* \left(\gamma_n^{(Q)} - \frac{k}{\hat{b}_{n,j,d}^{(r)} \mu_n} \right)}}{k! \left(1 + e^{-\delta(k - \hat{b}_{n,j,d}^{(r)} J_n)} \right) e^{-\delta(k - \hat{b}_{n,j,d}^{(r)} J_n)}}. \end{aligned} \quad (46)$$

Since Problem 14 is a convex problem, we obtain an optimal solution $\bar{\mathbf{v}}^{(r+1)}$ by using the interior point method [34]. Therefore, from (45), we can easily obtain the optimal solution $\bar{\mathbf{a}}_{d, \mathbf{T}^*}^{(r+1)}$ for given $\bar{\mathbf{v}}^{(r+1)}$. Then, we update the service caching distribution at iteration $r+1$, $\bar{\mathbf{a}}_d^{(r)}$, by

$$\hat{\mathbf{a}}_d^{(r+1)} = \hat{\mathbf{a}}_d^{(r)} + \alpha^{(r+1)} \left(\bar{\mathbf{a}}_{d, \mathbf{T}^*}^{(r+1)} - \hat{\mathbf{a}}_d^{(r)} \right). \quad (47)$$

Now, we solve the J approximate convex problems w.r.t. \mathbf{b}_j , $j \in \mathcal{J}$. The objective function in Problem 8 is separated into J sub-objective functions, i.e.,

$$\begin{aligned} \mathcal{H}_{j,d}(\mathbf{b}_j, \hat{a}_{j,d}^{(r)}, \mathbf{T}^*) = & \sum_{n \in \mathcal{N}_j} p_n P_n^{(U)}(\mathbf{T}^*) P_n^{(D)}(\mathbf{T}^*) \\ & \times \tilde{P}_{n,j,m}^{(Q)}(\mathbf{b}_j, \hat{a}_{j,d}^{(r)}), \quad j \in \mathcal{J}. \end{aligned} \quad (48)$$

Algorithm 2 Obtaining a near-optimal solution of Problem 2

-
- 1: Initialize \mathbf{T}^0 which is feasible to Problem 7, and set $r = 1$.
 - 2: **while** $\|\nabla \mathcal{P}_\infty(\mathbf{T}^{(r)})\|^2 \geq \tau$ **do**
 - 3: Obtain $\mathbf{T}^{(r)}$ according to (41).
 - 4: Set $r = r + 1$.
 - 5: Obtain $\bar{a}_{j,k}, j \in \mathcal{J}', k \in \{m, d\}$ according to (51).
 - 6: **if** $k = m$ **then**
 - 7: Obtain the near-optimal solution $\bar{\mathbf{b}}_m$ according to (43).
 - 8: Obtain $\bar{a}_{i,m}, j \in \mathcal{J} \setminus \mathcal{J}'$ by solving 11 using the interior point method.
 - 9: **else**
 - 10: Initialize $\mathbf{a}_d^0, \mathbf{b}_d^0$ which are feasible to Problem 8, and set $r = 1$.
 - 11: **while** $\|\nabla \mathcal{P}_d(\mathbf{a}, \mathbf{b}, \mathbf{T}^*)\|^2 \geq \tau$ **do**
 - 12: Obtain $\bar{a}_{j,d,\mathbf{T}^*}^{(r+1)}, j \in \mathcal{J} \setminus \mathcal{J}'$ by solving Problem 13 using the interior point method.
 - 13: Update $\hat{\mathbf{a}}_d^{(r)}$ according to (47).
 - 14: **for** $j \in \mathcal{J}$ **do**
 - 15: Obtain $\bar{\mathbf{b}}_{j,d,\mathbf{T}^*}^{(r+1)}$ by solving Problem 15 using the interior point method.
 - 16: Update $\hat{\mathbf{b}}_{j,d}^{(r)}$ according to 50.
 - 17: Set $r = r + 1$.
-

Then, for each $j \in \mathcal{J}$, we choose the approximation function of $\mathcal{H}_{j,d}(\mathbf{b}_j, \hat{a}_{j,d}^{(r)}, \mathbf{T}^*)$ by taking the second order Taylor expansion for \mathbf{b}_j , which is given by

$$\begin{aligned} \tilde{\mathcal{H}}_{j,d}(\mathbf{b}_j, \hat{a}_{j,d}^{(r)}, \hat{\mathbf{b}}_{j,d}^{(r)}, \mathbf{T}^*) &\triangleq -\mathbf{b}_j^T \mathbf{b}_j - \left(-2\hat{\mathbf{b}}_{j,d}^{(r)}\right. \\ &\quad \left. + \nabla_{\mathbf{b}_j} \mathcal{H}_{j,d}(\mathbf{b}_j, \hat{a}_{j,d}^{(r)}, \hat{\mathbf{b}}_{j,d}^{(r)}, \mathbf{T}^*) \Big|_{\mathbf{b}_{j,d}=\hat{\mathbf{b}}_{j,d}^{(r)}}\right)^T \mathbf{b}_j. \end{aligned} \quad (49)$$

Then, we formulate the following approximate convex problem w.r.t. $\mathbf{b}_j, j \in \mathcal{J}$.

Problem 15 (Approximate Problem 8 for \mathbf{b}_j at iteration $r + 1$):

$$\begin{aligned} \max_{\mathbf{b}_j} \quad & \tilde{\mathcal{H}}_{j,d}(\mathbf{b}_j, \hat{a}_{j,d}^{(r)}, \hat{\mathbf{b}}_{j,d}^{(r)}, \mathbf{T}^*) \\ \text{s.t.} \quad & (7), (8), (15). \end{aligned}$$

Since Problem 15 is a convex problem, we can obtain an optimal solution $\bar{\mathbf{b}}_{j,d}^{(r+1)}$ by using the interior point method [34]. Then, we update $\hat{\mathbf{b}}_{j,d}^{(r)}$ at iteration $r + 1$ by

$$\hat{\mathbf{b}}_{j,d}^{(r+1)} = \hat{\mathbf{b}}_{j,d}^{(r)} + \alpha^{(r+1)} \left(\bar{\mathbf{b}}_{j,d}^{(r+1)} - \hat{\mathbf{b}}_{j,d}^{(r)} \right), \quad j \in \mathcal{J}. \quad (50)$$

In the DT case, since the number of iterations for parallel SCA is constant [18], the complexity order is identical to that of each iteration in it. At each iteration, we solve one convex problem w.r.t. \mathbf{a} and J approximate convex problems w.r.t. $\mathbf{b}_j, j \in \mathcal{J}$, respectively. The computational complexity of solving the problem w.r.t. \mathbf{a} using the interior point method is $\mathcal{O}(N^{2+3K/2})$. On the other hand, the computational complexity of solving the problem w.r.t. \mathbf{b}_i using the interior point method is $\mathcal{O}(N^K K^{7/2})$. Finally, the total computational complexity is $\mathcal{O}(N^{2+3K/2})$. We can argue that the computational complexity of obtaining the near-optimal solution of Problem 8

is lower than that of obtaining the optimal solution of Problem 2.

Finally, we can obtain the near-optimal solution of Problem 8, as summarized in Algorithm 2. Note that some service combination probabilities are obviously determined from Corollary 1, specifically, $a_j = 0, j \in \mathcal{J}_n$ if $T_n = 0$ and $a_j = 0, j \notin \mathcal{J}_n$ if $T_n = 1$. Therefore, to reduce the computational complexity, we first obtain the near-optimal solution of service combination probability from Corollary 1 before solving the optimization problem.

$$\bar{a}_{j,k} = 0, \quad j \in \mathcal{J}', k \in \{m, d\}, \quad (51)$$

where $\mathcal{J}' \triangleq \cup_{n \in \mathcal{N} \setminus \{T_n^* = 0\}} \mathcal{J}_n \cup (\mathcal{J}_n \setminus \cup_{n \in \mathcal{N} \setminus \{T_n^* = 1\}} \mathcal{J}_n)$. Here, the near-optimal solution of the service combination probability from Corollary 1 is also summarized in Algorithm 2.

VI. NUMERICAL RESULTS

In this section, we show numerical results of the SSP given by Algorithms 1 and 2 for EC-enabled networks. Unless otherwise specified, we consider 10 latency sensitive services⁶ with the same computation workload size, i.e., $N = 10$ and $\frac{E_{j,n}}{f_n} = \mu, \forall n \in \mathcal{N}$. According to [3], [38], and [39], we set $K = 3, \lambda_{bs} = 5 \times 10^{-4}$ node/m², $\lambda_u = 3 \times 10^{-3}$ node/m², $W = 10$ MHz, $f_n = 3 \times 10^5$ Cycles, $\delta = 100, \omega = 1000, S_n^{(i)} = 420$ KB, $S_n^{(o)} = 42$ KB, $p_s = 1, \kappa = 30, \tau = 10^{-4}, \alpha = 4, \gamma_n^{(U)} = 0.84$ s, $\gamma_n^{(D)} = 84$ ms, and $\gamma_n^{(Q)} = 1$ s, unless otherwise specified. We assume that users' service preference follows the Zipf distribution, i.e., $p_n = \frac{n^\epsilon}{\sum_{n \in \mathcal{N}} n^\epsilon}$, where the Zipf exponent is $\epsilon = 1.1$ [16], [40]. To assess the performance of the proposed algorithms, we consider the following baseline schemes:

- *Uniform service caching and proportional computation resource allocation (UCPS) scheme* : The service caching distribution \mathbf{a} follows the uniform distribution [41], and the computing resource allocation \mathbf{b} is proportional to users' service preference.
- *Geography-based service caching and proportional computation resource allocation (GCPS) scheme* : The service probability \mathbf{T} is determined by users' service preference, i.e., $T_n = p_n$, and \mathbf{a} is determined by the optimal geographic method in [35]. Similar to the UCPS scheme, \mathbf{b} is proportional to users' service preference.
- *Transmission performance-based service caching and proportional computation resource allocation (TCPS) scheme* : \mathbf{a} is optimized by considering the downlink transmission performance as in [16], and \mathbf{b} is proportional to users' service preference.
- *Popularity-based service caching and optimal computation resource allocation (PCOS) scheme* : Each BS selects K most popular service software [42]. The computation resource allocation \mathbf{b} is optimized using Algorithm 1 for given \mathbf{a} .

⁶Note that 10 service types and 5 ~ 8 BSs' cache sizes (i.e., $N = 10$ and $K = 5 \sim 8$) are considered as most existing works on service caching such as [3], [11]–[13], [15]. However, our algorithm can be applicable for larger N and K with reasonably small execution time such as 0.4982 second with $N = 500$ and $K = 50$ for Algorithm 2.

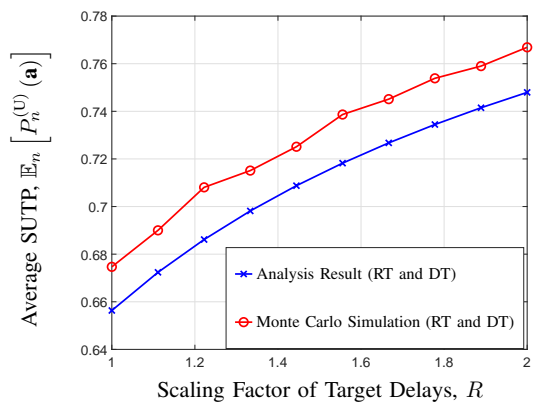
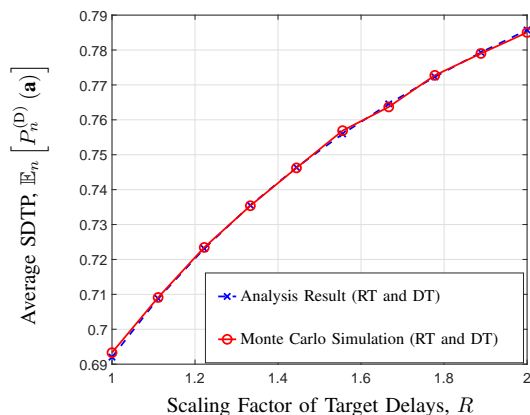
(a) Successful uplink transmission, $P_n^{(U)}(\mathbf{a})$ (b) Successful downlink transmission, $P_n^{(D)}(\mathbf{a})$

Fig. 2. Average SUTP $\mathbb{E}_n [P_n^{(U)}(\mathbf{a})]$ and SDTP $\mathbb{E}_n [P_n^{(D)}(\mathbf{a})]$ as a function of the scaling factor of target delays R with $F_{bs} = 7.5 \times 10^6$ Cycles/s.

Note that to the best of our knowledge, none of the previous works have jointly optimized \mathbf{a} and \mathbf{b} . Therefore, we compare the proposed algorithms with the works above that optimize the content caching probability based on users' service preference.

Figure 2 shows the impact of target delays on the average SUTP in (13) and the average SDTP in (14). Here, the scaling factor of the target delays, R , is introduced, to investigate the impact of target delays on uplink and downlink transmissions. Specifically, for given initial target delays $\gamma_o^{(U)}$, $\gamma_o^{(Q)}$, and $\gamma_o^{(D)}$, the target delays are determined as $\gamma_n^{(U)} = R\gamma_o^{(U)}$, $\gamma_n^{(Q)} = R\gamma_o^{(Q)}$, and $\gamma_n^{(D)} = R\gamma_o^{(D)}$. From Fig. 2(a), we can see that the simulation results of the SUTP have the similar trend to the analysis results of the SUTP. However, there is a performance gap between the simulation results and the analysis results, caused by the uplink transmission assumption in Section III. On the other hand, in the case of SDTP, Fig. 2(b), we can see that the simulation results show a good agreement with the analysis results as no assumption is used for the analysis.

Figure 3 shows the average SCPP according to R . In Fig. 3, 'Analysis Result (RT)' refers to the RT case in (17), 'Analysis Result (DT)' refers to the DT case in (18), and 'Approximate

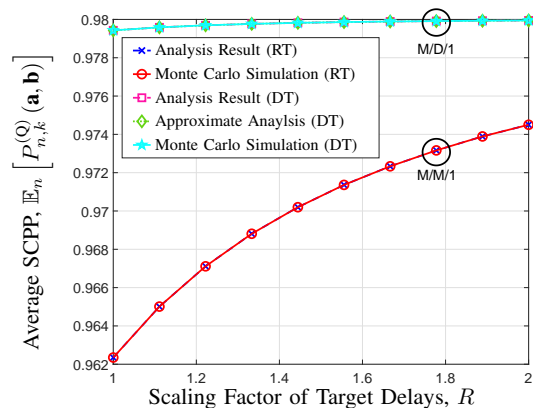


Fig. 3. Average SCPPs $\mathbb{E}_n [P_{n,m}^{(Q)}(\mathbf{a}, \mathbf{b})]$ (RT) and $\mathbb{E}_n [P_{n,d}^{(Q)}(\mathbf{a}, \mathbf{b})]$ (DT) as a function of the scaling factor of target delays R with $F_{bs} = 7.5 \times 10^6$ Cycles/s.

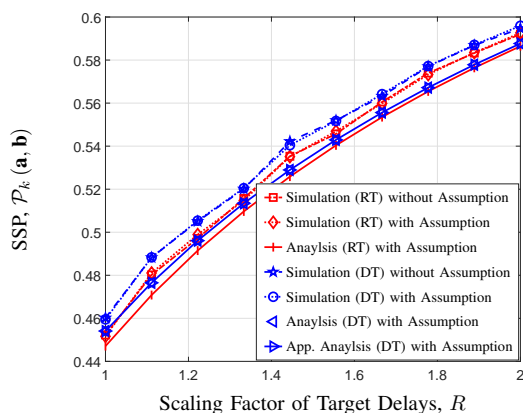
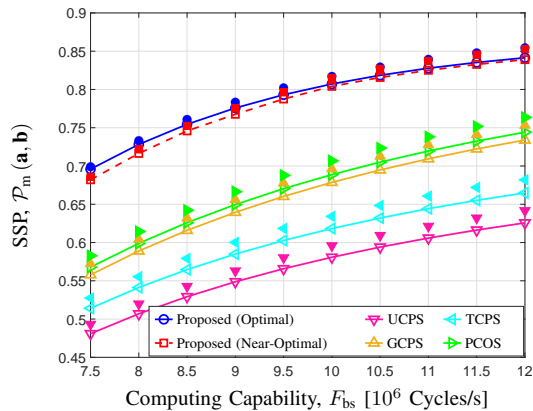


Fig. 4. Successful service probabilities, \tilde{P}_m (RT) and \tilde{P}_d (DT), as a function of the scaling factor of target delays R with $F_{bs} = 7.5 \times 10^6$ Cycles/s.

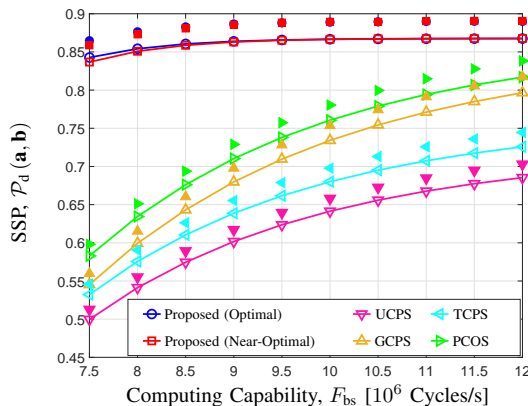
Analysis (DT)' refers to the approximated SCPP of DT case in (20). From Fig. 3, we can see that there is no performance gap between the approximated analysis result in (20) and the analysis result in (18) for the DT case. This is because, as mentioned in Section II, the gap between the original indicator function and the logistic sigmoid function is small. Moreover, from Fig. 3, we can see that the simulation results of RT and DT cases have the similar trend to the analysis results as no assumption is used for the analysis.

Figure 4 shows the SSPs for RT and DT cases in (22) and (23) according to R . Here, the simulation and analysis results 'with Assumption' refer to the approximated SSP in (12) while those 'without Assumption' refer to the SSP in (11). From Fig. 4, we can see that the simulation results of (11) show a good agreement with those of (12). Therefore, we can see that the performance gap, caused by the independence assumption, is ignorably small. Furthermore, from Fig. 4, we can see that the simulation results of the SSP for both the RT and DT cases also have a similar trend to the analysis results of the SSP.

Figure 5 shows the SSP for EC-enabled networks versus the computing capability of the EC server, F_{bs} . Here, the



(a) Random Service Time



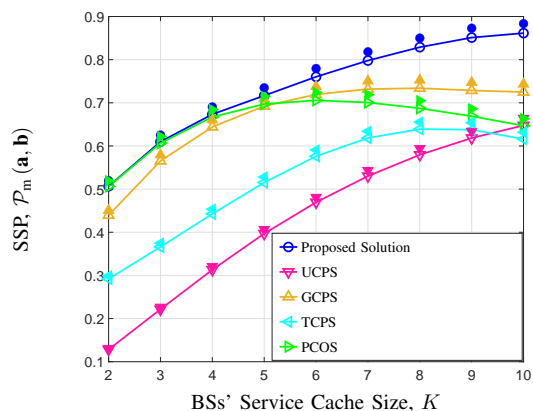
(b) Deterministic Service Time

Fig. 5. Successful service probabilities, $\tilde{\mathcal{P}}_m$ (RT) and $\tilde{\mathcal{P}}_d$ (DT), as a function of the computing capability F_{bs} with $K = 8$. The filled symbols represent the simulation results of the SSP for two cases.

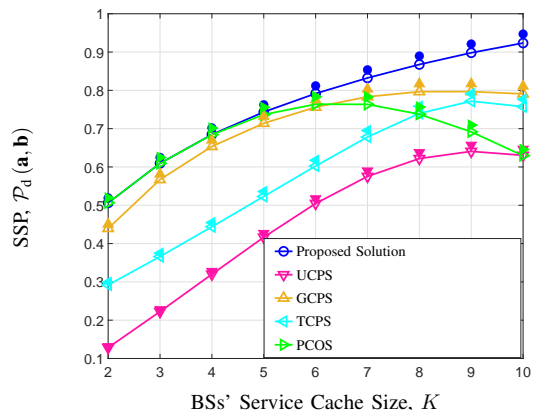
optimal and near-optimal solutions are obtained by Algorithms 1 and 2, respectively. We can see that our proposed solutions outperform the baseline schemes. Moreover, we can see that the performance gap between the optimal solution and near-optimal solution decreases with F_{bs} . In other words, the near-optimal solution achieves reliable performance especially when F_{bs} is high. In addition, we can see that the SSP of each scheme converges to different points with increasing F_{bs} . This is because the SCPP is always 1 due to the sufficiently high computing capability of the EC server F_{bs} , while the SUTP and SDTP have a different values depending on the service caching distribution \mathbf{a} .

From Fig. 4. and Fig. 5., we can see that the SSP increases with R and F_{bs} . Moreover, the SSP in the DT case is always higher than the SSP in the RT case due to the randomness of computation time in the RT case.

Figure 6 shows the SSP for EC-enabled networks versus the BSs' service caching storage K . From Fig. 6, we can see that the SSP of each baseline scheme first increases and then decreases with the BSs' cache size K . For the small K , as K increases, there can be larger number of BSs, which store the requested service software, and this leads to the high SUTP and SDTP. Consequently, the SSP increases. However, as K



(a) Random Service Time



(b) Deterministic Service Time

Fig. 6. Successful service probabilities, $\tilde{\mathcal{P}}_m$ (RT) and $\tilde{\mathcal{P}}_d$ (DT), as a function of the BSs' service cache size K with $F_{bs} = 1.2 \times 10^7$ Cycles/s. The filled symbols represent the simulation results of the SSP for two cases.

keeps increasing, the computing capability assigned for each service software at a EC server decreases due to the limited computing capability. Since baseline schemes do not jointly consider the service caching distribution and the computing resource allocation, the computation time monotonically increases with K , which results in low SCPP compared to the SUTP and the SDTP. As a result, the SSP decreases. On the other hand, from Fig. 6, we can see that the SSP of the proposed solution keeps increasing with K due to the joint optimization of service caching distribution and the computing resource allocation.

Furthermore, from Fig. 5 and Fig. 6, we can see that the proposed solutions outperform the baseline schemes even when the SSP is high, e.g., when $F_{bs} \geq 10^7$ Cycles/s and $K \geq 9$.

Figure 7 shows the impact of computing capability of the EC server F_{bs} and the BSs' service caching storage K on the SSP with large number of services ($N = 100$). Since it is hard to obtain the optimal solution due to the computational complexity, we only show the near-optimal solution obtained by Algorithm 2. From Fig. 7, we can observe that the proposed solution outperforms all the baseline schemes. Specifically, in Fig. 7, when F_{bs} is low, some baseline schemes are not feasible

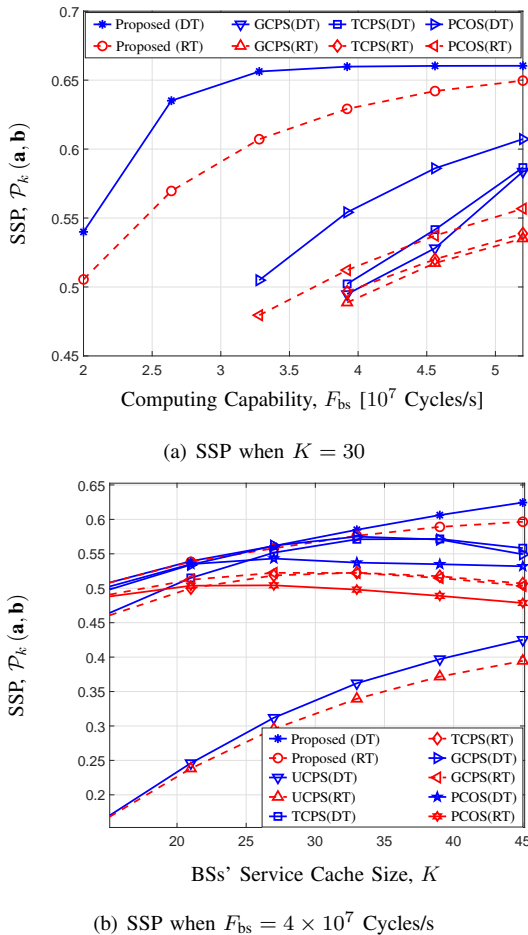


Fig. 7. Successful service probabilities, \tilde{P}_m (RT) and \tilde{P}_d (DT), as a function of the BSs' service cache size K and the computing capability F_{bs} with $N = 100$.

as they cannot satisfy the stability condition of the service queue. However, the proposed solution satisfies the stability condition of the service queue regardless of F_{bs} . Moreover, as the SSP increases with F_{bs} and K , we can see that the near-optimal solution can be applied to EC-enabled networks with large number of services.

VII. CONCLUSION

In this paper, we develop an efficient service caching and a computing resource allocation in EC enabled networks with multiple types of latency sensitive services. Specifically, we derive the closed form expression of the SSP in both the RT and DT cases. Then, to maximize the SSP, we formulate optimization problems of the service caching distribution and the computing resource allocation in both cases, which are challenging nonconvex problems. We propose an iterative algorithm to obtain a stationary point of the SSP maximization problem. Then, in the high computing capability region, we formulate the asymptotic SSP maximization problem and obtain the stationary point of the asymptotic SSP maximization problem. Furthermore, we develop an iterative algorithm with low complexity to obtain a near-optimal solution of the SSP maximization problem. Finally, from numerical simulations,

we show that the proposed solutions in both the general and high computing capability regions achieve higher SSP than that of the baseline schemes. Moreover, the near-optimal solution in the high computing capability region achieves a reliable performance compared to the optimal solution in the general region. Then, we show that the SSP increases with the target delays, the computing capability of EC servers, and BSs' service cache size in both the RT and DT cases. We also show the near-optimal solution can be applied for the EC enabled networks that have large number of services.

APPENDIX

A. Proof of Lemma 1

By relaxing computing constraints in (8), we obtain Lagrange function $L(\mathbf{b}_j, \eta_j)$, $j \in \mathcal{J}$ by

$$L(\mathbf{b}_j, \eta_j) = \sum_{n \in \mathcal{N}_j} \frac{p_n T_{n,m}^{(r)} a_{j,m}^{(r)} e^{\lambda_{n,m}^{(r)} \gamma_n^{(Q)} - b_{n,j} J_n}}{D_n (T_{n,m}^{(r)})^2 + E_n T_{n,m}^r + A_n^2} - \frac{1}{\omega} \phi_{n,j}(\mathbf{a}_m^{(r)}, b_{n,j}) + \eta_j \left(\sum_{j \in \mathcal{J}_n} b_{n,j} - 1 \right), \quad (52)$$

where η_j is the Lagrange multiplier w.r.t. the constraint in (8). Then, we obtain the derivative of the Lagrange function given by

$$\frac{\partial L(\mathbf{b}_j, \eta_j)}{\partial b_{n,j}} = - \frac{J_n p_n T_{n,m}^{(r)} a_{j,m}^{(r)} e^{\lambda_{n,m}^{(r)} \gamma_n^{(Q)} - b_{n,j} J_n}}{D_n (T_{n,m}^{(r)})^2 + E_n T_{n,m}^r + A_n^2} - \frac{\mu_n}{\omega} e^{\phi_{n,j}(\mathbf{a}_m^{(r)}, b_{n,j})} + \eta_j, j \in \mathcal{J}. \quad (53)$$

We obtain the KKT conditions by (7), (8), and

$$\frac{\partial L(\mathbf{b}_j, \eta_j)}{\partial b_{n,j}} = 0, \quad j \in \mathcal{J}. \quad (54)$$

Since the strong condition holds, by substituting (53) into (54), we obtain

$$G_{n,j}(b_{n,j}) = \eta_j, \quad (55)$$

where $G_{n,j}(b_{n,j})$ is given by

$$G_{n,j}(b_{n,j}) = \frac{J_n p_n T_{n,m}^{(r)} a_{j,m}^{(r)} e^{\lambda_{n,m}^{(r)} \gamma_n^{(Q)} - b_{n,j} J_n}}{D_n (T_{n,m}^{(r)})^2 + E_n T_{n,m}^r + A_n^2} + \frac{\mu_n}{\omega} e^{\phi_{n,j}(\mathbf{a}_m^{(r)}, b_{n,j})}. \quad (56)$$

By considering (7), (8), and (56), we represent the optimal solution $\bar{b}_{n,j,m}^{(r+1)}$, by (30).

B. Proof of Lemma 5

First, by relaxing the constraint in (8), we obtain the Lagrange function $L(\mathbf{b}_j, \zeta_j)$, $j \in \mathcal{J}$ by

$$L(\mathbf{b}_j, \zeta_j) = \sum_{n \in \mathcal{N}_j} \frac{p_n T_n^* e^{\lambda_n^* \gamma_n^{(Q)} - b_{n,j} J_n}}{D_n (T_n^*)^2 + E_n T_n^* + A_n^2} + \zeta_j \left(1 - \sum_{j \in \mathcal{J}_n} b_{n,j} \right), \quad (57)$$

where ζ_j is the Lagrange multiplier w.r.t. the constraint in (8). Then, we obtain the derivative of Lagrange function given by

$$\frac{\partial L(\mathbf{b}_j, \zeta_j)}{\partial b_{n,j}} = \frac{-J_n p_n T_n^* e^{\lambda_n^* \gamma_n^{(Q)} - b_{n,j} J_n}}{D_n (T_n^*)^2 + E_n T_n^* + A_n^2} + \zeta_j, \quad j \in \mathcal{J}. \quad (58)$$

We obtain the KKT conditions by (7), (8), and

$$\frac{\partial L(\mathbf{b}_j, \zeta_j)}{\partial b_{n,j}} = 0, \quad j \in \mathcal{J}. \quad (59)$$

Since the strong condition holds, by substituting (58) into (59), we obtain $b_{n,j}$, $j \in \mathcal{J}$ by

$$\bar{b}_{n,j,m} = \frac{1}{J_n} \left\{ \lambda_n^* \gamma_n^{(Q)} + \log \left(\frac{J_n p_n T_n^*}{\hat{\zeta}_j (D_n (T_n^*)^2 + E_n T_n^* + A_n^2)} \right) \right\}. \quad (60)$$

By considering (7), (8), and (59), for $n \in \mathcal{N}_j$, $j \in \mathcal{J}$, we represent the optimal solution $\bar{b}_{n,j,m}$, which is given by

$$\bar{b}_{n,j,m} = \max \left\{ \left(\log \left(\frac{J_n p_n T_n^*}{\hat{\zeta}_j (D_n (T_n^*)^2 + E_n T_n^* + A_n^2)} \right) \right) \times \frac{1}{J_n} + \frac{\lambda_n^*}{\mu_n}, \frac{\lambda_n^*}{\mu_n} \right\}. \quad (61)$$

Next, we suppose that for all $n \in \mathcal{N}_j$ and $j \in \mathcal{J}$, the optimal solution $\bar{b}_{n,j,m}$ is constructed only by the first term in the max function of (61), which is represented by

$$\bar{b}_{n,j,m} = \frac{1}{J_n} \log \left(\frac{J_n p_n (T_n^*)^2}{\hat{\zeta}_j (D_n T_n^* + E_n T_n^* + A_n^2)} \right) + \frac{\lambda_n^*}{\mu_n}. \quad (62)$$

Then, we can obtain the closed form expression of the Lagrangian multiplier $\hat{\zeta}_j^*$, which satisfies $\sum_{n \in \mathcal{N}_j} \bar{b}_{n,j,m} = 1$, $j \in \mathcal{J}$, by

$$\hat{\zeta}_j^* = e^{\frac{-1 + \sum_{n \in \mathcal{N}_j} \frac{1}{J_n} \left(\lambda_n^* \gamma_n^{(Q)} + \log \left(\frac{J_n p_n T_n^*}{D_n (T_n^*)^2 + E_n T_n^* + A_n^2} \right) \right)}{\sum_{n \in \mathcal{N}_j} \frac{1}{J_n}}}. \quad (63)$$

By substituting $\hat{\zeta}_j^*$ into $\hat{\zeta}_j$ in (61), we can rewrite the optimal solution $b_{n,j}^*$ as follows.

$$\bar{b}_{n,j,m} = \max \left\{ \left(\log \left(\frac{J_n p_n T_n^*}{\hat{\zeta}_j^* (D_n (T_n^*)^2 + E_n T_n^* + A_n^2)} \right) \right) \times \frac{1}{J_n} + \frac{\lambda_n^*}{\mu_n}, \frac{\lambda_n^*}{\mu_n} \right\}, \quad n \in \mathcal{N}_j, \quad j \in \mathcal{J}. \quad (64)$$

Then, we can rewrite $\log \left(\frac{J_n p_n T_n^*}{\hat{\zeta}_j^* (D_n (T_n^*)^2 + E_n T_n^* + A_n^2)} \right)$, $n \in \mathcal{N}$ as follow

$$\begin{aligned} & \log \left(\frac{J_n p_n T_n^*}{\hat{\zeta}_j^* (D_n (T_n^*)^2 + E_n T_n^* + A_n^2)} \right) \\ &= \frac{1 - \sum_{n \in \mathcal{N}_j} \frac{\lambda_n^*}{\mu_n} + \sum_{k \in \mathcal{N}_j} \frac{G_{n,k}}{J_k}}{\sum_{n \in \mathcal{N}_j} \frac{1}{J_n}}, \end{aligned} \quad (65)$$

where $G_{n,k} = \log \left(\frac{J_n p_n T_n^*}{(D_n (T_n^*)^2 + E_n T_n^* + A_n^2)} \right) - \log \left(\frac{J_k p_k T_k^*}{(D_k (T_k^*)^2 + E_k T_k^* + A_k^2)} \right)$.

Since $\frac{\log \left(\frac{J_n p_n T_n^*}{\hat{\zeta}_j^* (D_n (T_n^*)^2 + E_n T_n^* + A_n^2)} \right)}{J_n} \leq 1 - \sum_{n \in \mathcal{N}_j} \frac{\lambda_n^*}{\mu_n} + \frac{1}{J_n} \log(\zeta_j) - \frac{\lambda_n^*}{\mu_n}$, and $\sum_{k \in \mathcal{N}_j} \frac{G_{n,k}}{J_k} \geq -1 + \sum_{n \in \mathcal{N}_j} \frac{\lambda_n^*}{\mu_n}$, the

condition in (65) is always greater than 0. Therefore, the optimal solution in (64) is always greater than $\frac{\lambda_n^*}{\mu_n}$. Therefore, we can remove the max function and obtain the closed form optimal solution given by (43).

REFERENCES

- [1] M. Kim, H. Cho, Y. Cui, and J. Lee, "Service caching and computation resource allocation for large-scale edge computing-enabled networks," in *Proc. IEEE Glob. Commun. Conf. (GLOBECOM)*, Taipei, Taiwan, Dec. 2020, pp. 1–6.
- [2] Y. Mao, C. You, J. Zhang, K. Huang, and K. B. Letaief, "A survey on mobile edge computing: The communication perspective," *IEEE Commun. Surveys Tuts.*, vol. 19, no. 4, pp. 2322–2358, Aug. 2017.
- [3] J. Xu, L. Chen, and P. Zhou, "Joint service caching and task offloading for mobile edge computing in dense networks," in *Proc. IEEE Conf. Comput. Commun. (INFOCOM)*, Honolulu, HI, USA, Apr. 2018, pp. 1–9.
- [4] T. X. Tran and D. Pompili, "Joint task offloading and resource allocation for multi-server mobile-edge computing networks," *IEEE Trans. Veh. Technol.*, vol. 68, no. 1, pp. 856–868, Nov. 2018.
- [5] C.-F. Liu, M. Bennis, M. Debbah, and H. V. Poor, "Dynamic task offloading and resource allocation for ultra-reliable low-latency edge computing," *IEEE Trans. Commun.*, vol. 67, no. 6, pp. 4132–4150, Feb. 2019.
- [6] Y. Mao, J. Zhang, and K. B. Letaief, "Dynamic computation offloading for mobile-edge computing with energy harvesting devices," *IEEE J. Sel. Areas Commun.*, vol. 34, no. 12, pp. 3590–3605, Sep. 2016.
- [7] Y. Mao, J. Zhang, and K. B. Letaief, "Joint task offloading scheduling and transmit power allocation for mobile-edge computing systems," in *Proc. IEEE Wireless Commun. Netw. Conf. (WCNC)*, San Francisco, CA, USA, Mar. 2017, pp. 1–6.
- [8] H. Hu, P. Zong, H. Wang, and H. Zhu, "Performance analysis for D2D-enabled cellular networks with mobile edge computing," in *Proc. Int. Conf. Wireless Commun. Signal Process. (WCSP)*, Xi'an, China, Oct. 2019, pp. 1–6.
- [9] C. Park and J. Lee, "Mobile edge computing-enabled heterogeneous networks," *IEEE Trans. Wireless Commun.*, vol. 20, no. 2, pp. 1038–1051, Oct. 2020.
- [10] S.-W. Ko, K. Han, and K. Huang, "Wireless networks for mobile edge computing: Spatial modeling and latency analysis," *IEEE Trans. Wireless Commun.*, vol. 17, no. 8, pp. 5225–5240, Jun. 2018.
- [11] T. X. Tran, K. Chan, and D. Pompili, "Costa: Cost-aware service caching and task offloading assignment in mobile-edge computing," in *Proc. IEEE Int. Conf. Sens., Commun., Netw. (SECON)*, Boston, MA, USA, Jun. 2019, pp. 1–9.
- [12] J. Li, H. Zhang, H. Ji, and X. Li, "Joint computation offloading and service caching for MEC in multi-access networks," in *Proc. IEEE Int. Symp. Pers., Indoor Mob. Radio Commun. (PIMRC)*, Istanbul, Turkey, Sep. 2019, pp. 1–6.
- [13] M. Chen, Y. Hao, L. Hu, M. S. Hossain, and A. Ghoneim, "Edge-CoCaCo: Toward joint optimization of computation, caching, and communication on edge cloud," *IEEE Wireless Commun.*, vol. 25, no. 3, pp. 21–27, Jul. 2018.
- [14] T. Zhao, I.-H. Hou, S. Wang, and K. Chan, "Red/LeD: An asymptotically optimal and scalable online algorithm for service caching at the edge," *IEEE J. Sel. Areas Commun.*, vol. 36, no. 8, pp. 1857–1870, Jun. 2018.
- [15] W. Wen, Y. Cui, T. Q. Quek, F.-C. Zheng, and S. Jin, "Joint optimal software caching, computation offloading and communications resource allocation for mobile edge computing," *IEEE Trans. Veh. Technol.*, vol. 69, no. 7, pp. 7879–7894, May 2020.
- [16] Y. Cui and D. Jiang, "Analysis and optimization of caching and multicasting in large-scale cache-enabled heterogeneous wireless networks," *IEEE Trans. Wireless Commun.*, vol. 16, no. 1, pp. 250–264, Oct. 2016.
- [17] S. Markov, N. Kyurkchiev, A. Iliev, and A. Rahnev, "On the approximation of the generalized cut functions of degree $p+1$ by smooth hyper-log-logistic function," *Dyn. Syst. Appl.*, vol. 27, no. 4, pp. 715–728, Aug. 2018.
- [18] M. Razaviyayn, M. Hong, Z.-Q. Luo, and J.-S. Pang, "Parallel successive convex approximation for nonsmooth nonconvex optimization," in *Proc. Neural Inf. Process. (NIPS)*, Montreal, QC, Canada, Dec. 2014, pp. 1–9.
- [19] H. ElSawy, A. Sultan-Salem, M.-S. Alouini, and M. Z. Win, "Modeling and analysis of cellular networks using stochastic geometry: A tutorial," *IEEE Commun. Surveys Tuts.*, vol. 19, no. 1, pp. 167–203, Nov. 2016.

- [20] D. T. Marr, F. Binns, D. L. Hill, G. Hinton, D. A. Koufaty, J. A. Miller, and M. Upton, "Hyper-threading technology architecture and microarchitecture." *Intel Technol. J.*, vol. 6, no. 1, pp. 1–12, Feb. 2002.
- [21] X. Ma, A. Zhou, S. Zhang, and S. Wang, "Cooperative service caching and workload scheduling in mobile edge computing," in *Proc. IEEE Conf. Comput. Commun. (INFOCOM)*, Toronto, ON, Canada, Jul. 2020, pp. 2076–2085.
- [22] R. Fantacci and B. Picano, "Performance analysis of a delay constrained data offloading scheme in an integrated cloud-fog-edge computing system," *IEEE Trans. Veh. Technol.*, vol. 69, no. 10, pp. 12 004–12 014, Oct. 2020.
- [23] Q. Kuang, J. Gong, X. Chen, and X. Ma, "Analysis on computation-intensive status update in mobile edge computing," *IEEE Trans. Veh. Technol.*, vol. 69, no. 4, pp. 4353–4366, Apr. 2020.
- [24] A. Abhari and M. Soraya, "Workload generation for youtube," *Multimedia Tools and Applications*, vol. 46, no. 1, pp. 91–118, Jun. 2010.
- [25] F. Chiariotti, O. Vikhrova, B. Soret, and P. Popovski, "Peak age of information distribution for edge computing with wireless links," *IEEE Trans. Commun.*, vol. 69, no. 5, pp. 3176–3191, May 2021.
- [26] J. Zhang and O. Simeone, "On model coding for distributed inference and transmission in mobile edge computing systems," *IEEE Commun. Lett.*, vol. 23, no. 6, pp. 1065–1068, Jun. 2019.
- [27] Q. Zhang, J. Chen, L. Ji, Z. Feng, Z. Han, and Z. Chen, "Response delay optimization in mobile edge computing enabled uav swarm," *IEEE Trans. Veh. Technol.*, vol. 69, no. 3, pp. 3280–3295, Mar. 2020.
- [28] X. Qin, Z. Song, Y. Hao, and X. Sun, "Joint resource allocation and trajectory optimization for multi-uav-assisted multi-access mobile edge computing," *IEEE Commun. Lett.*, vol. 10, no. 7, pp. 1400–1404, Jul. 2021.
- [29] C. You, K. Huang, H. Chae, and B.-H. Kim, "Energy-efficient resource allocation for mobile-edge computation offloading," *IEEE Transactions on Wireless Communications*, vol. 16, no. 3, pp. 1397–1411, Mar. 2016.
- [30] T. D. Novlan, H. S. Dhillon, and J. G. Andrews, "Analytical modeling of uplink cellular networks," *IEEE Trans. Wireless Commun.*, vol. 12, no. 6, pp. 2669–2679, May 2013.
- [31] S. Singh, H. S. Dhillon, and J. G. Andrews, "Offloading in heterogeneous networks: Modeling, analysis, and design insights," *IEEE Trans. Wireless Commun.*, vol. 12, no. 5, pp. 2484–2497, Apr. 2013.
- [32] L. Kleinrock, "Theory, volume 1, queueing systems," 1975.
- [33] G. J. Franx, "A simple solution for the m/d/c waiting time distribution," *Oper. Res. Lett.*, vol. 29, no. 5, pp. 221–229, Dec. 2001.
- [34] S. Boyd and L. Vandenberghe, *Convex Optimization*. Cambridge, UK: Cambridge University Press, 2004.
- [35] B. Blaszczyszyn and A. Giovanidis, "Optimal geographic caching in cellular networks," in *Proc. IEEE Int. Conf. Commun. (ICC)*, London, UK, Jun. 2015, pp. 1–6.
- [36] H. A. Le Thi and T. P. Dinh, "DC programming and DCA: Thirty years of developments," *Math. Prog.*, vol. 169, no. 1, pp. 5–68, Jan. 2018.
- [37] B. K. Sriperumbudur and G. R. Lanckriet, "On the convergence of the concave-convex procedure," in *Proc. Neural Inf. Process. Syst. (NIPS)*, Vancouver, BC, Canada, Dec. 2009, pp. 1–9.
- [38] S. Bi, L. Huang, and Y.-J. A. Zhang, "Joint optimization of service caching placement and computation offloading in mobile edge computing systems," *IEEE Trans. Wireless Commun.*, vol. 19, no. 7, pp. 4947–4963, Apr. 2020.
- [39] J. Ren, G. Yu, Y. He, and G. Y. Li, "Collaborative cloud and edge computing for latency minimization," *IEEE Trans. Veh. Technol.*, vol. 68, no. 5, pp. 5031–5044, Mar. 2019.
- [40] J. Kwak, Y. Kim, L. B. Le, and S. Chong, "Hybrid content caching in 5G wireless networks: Cloud versus edge caching," *IEEE Trans. Wireless Commun.*, vol. 17, no. 5, pp. 3030–3045, May 2018.
- [41] S. Tamoor-ul Hassan, M. Bennis, P. H. Nardelli, and M. Latva-Aho, "Modeling and analysis of content caching in wireless small cell networks," in *Proc. IEEE Int. Symp. Wireless Commun. Syst. (ISWCS)*, Brussels, Belgium, Aug. 2015, pp. 1–5.
- [42] E. Baştuğ, M. Bennis, and M. Debbah, "A transfer learning approach for cache-enabled wireless networks," in *Proc. Int. Symp. Modeling Optim. Mob. Ad Hoc, Wireless Netw. (WiOpt)*, Mumbai, India, May 2015, pp. 1–6.